
Drell-Yan lepton angular dependencies at the LHC

D. Bachas¹ on behalf of the ATLAS, CMS and LHCb collaborations

¹INFN Lecce

Transversity 2017 at Frascati

December 13, 2017

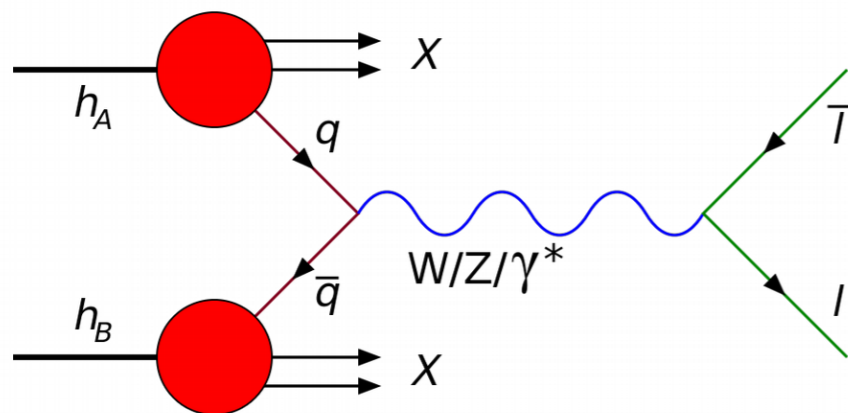


- Angular coefficients in Z-boson events
 - ATLAS (JHEP08(2016)159)
 - CMS (Phys. Lett. B 750 (2015) 154)
- φ^* measurement
 - ATLAS: (Eur. Phys. J. C 76(5), 1-61 (2016))
 - CMS: arXiv:1710.07955(CMS-SMP-17-002), (CMS PAS SMP-15-011)
 - LHCb: (JHEP 09 (2016) 136), JHEP01(2016)155, JHEP05(2015)109, JHEP08(2015)039, JHEP02(2013)106
- Measurement of A_{FB} and $\sin^2\theta_W^{\text{eff}}$
 - ATLAS: (JHEP 09 (2015) 049), arXiv:1710.05167v1
 - CMS: (CMS PAS SMP-16-007)
 - LHCb: (JHEP 1511(2015) 190)

Focus on most recent results

Introduction

- The Drell Yan process denotes the: “Massive lepton pair production in hadron-hadron collisions at high energies” (Phys. Rev.Lett.25, 316 (1970))
- The Drell-Yan mechanism was proposed and observed in 1970. It was a milestone in the building of QCD as the theory of the strong interaction
- In 1983 lead to the discovery of W and Z bosons, which confirmed the theory of the electroweak unification
- After ~47 years, is this process still of interest and what can we learn from it?



MASSIVE LEPTON-PAIR PRODUCTION IN HADRON-HADRON COLLISIONS AT HIGH ENERGIES*

Sidney D. Drell and Tung-Mow Yan

Stanford Linear Accelerator Center, Stanford University, Stanford, California 94305

(Received 25 May 1970)

On the basis of a parton model studied earlier we consider the production process of large-mass lepton pairs from hadron-hadron inelastic collisions in the limiting region, $s \rightarrow \infty$, Q^2/s finite, Q^2 and s being the squared invariant masses of the lepton pair and the two initial hadrons, respectively. General scaling properties and connections with deep inelastic electron scattering are discussed. In particular, a rapidly decreasing cross section as $Q^2/s \rightarrow 1$ is predicted as a consequence of the observed rapid falloff of the inelastic scattering structure function νW_2 near threshold.

Phys.Rev.Lett. 25 (1970) 316-320

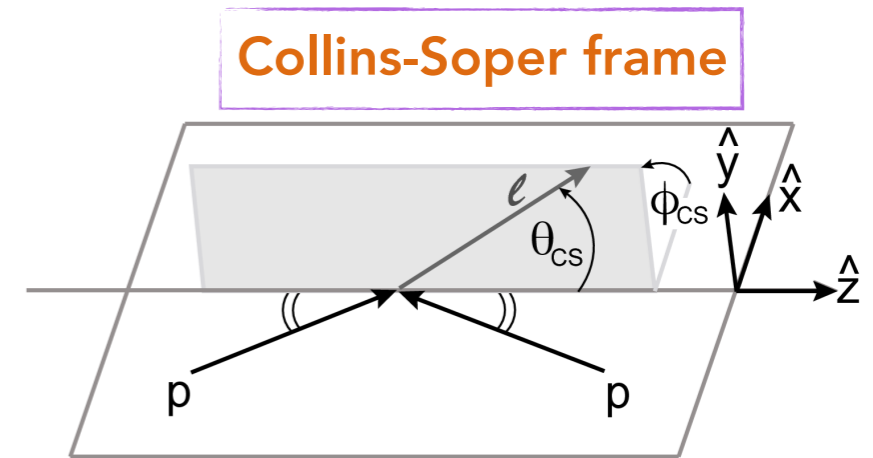
Motivation

- The Drell-Yan process at the LHC nowadays allows:
 - Stress testing of the factorization theorem at higher energies
 - Probing the proton PDFs, by e.g providing valuable information on the d-valence PDF and unique information of the light sea decomposition
 - Measuring fundamental electroweak parameters
 - Searching for new physics in high dilepton mass final states

Angular coefficients in Z-boson events

Angular distributions of charged lepton pairs in Drell–Yan

- Angular distributions provide a way to study the D-Y QCD production dynamics through spin correlation effects between the initial-state partons and the final-state leptons
 - mediated by a spin-1 intermediate state, predominantly the Z boson.
- Define lepton polar and azimuthal angular variables ($\cos\theta$ and φ) in Collins-Soper frame
- The full five-dimensional differential cross-section can be decomposed as a sum of 9 harmonic polynomials $P_i(\cos\theta, \varphi)$ multiplied by corresponding helicity cross-sections that depend on p_{TZ}, y_Z, m_Z
 - factorize out the unpolarized cross-section (σ_{U+L})
 - dimensionless angular coefficients $A_0-7(p_{TZ}, y_Z, m_Z)$: ratios of helicity cross-sections with respect to the unpolarized one



- Rest frame of the dilepton system
- z-axis bisecting directions of incoming proton momenta
- Direction of z-axis defined by longitudinal boost of di-lepton system in the Lab.frame

$$\frac{d\sigma}{dp_T^Z dy^Z dm^Z d\cos\theta d\phi} = \frac{3}{16\pi} \frac{d\sigma^{U+L}}{dp_T^Z dy^Z dm^Z} \left\{ (1 + \cos^2\theta) + \frac{1}{2} A_0(1 - 3\cos^2\theta) + A_1 \sin 2\theta \cos\phi + \frac{1}{2} A_2 \sin^2\theta \cos 2\phi + A_3 \sin\theta \cos\phi + A_4 \cos\theta + A_5 \sin^2\theta \sin 2\phi + A_6 \sin 2\theta \sin\phi + A_7 \sin\theta \sin\phi \right\}$$

Angular coefficients

- All hadronic dynamics from the production mechanism are described implicitly within the structure of the A_i coefficients.
 - They are extracted from the shapes of the angular distributions
 - The weighted average of angular distributions with respect to some polynomial isolates an average reference value or moment of its corresponding A_i
- At LO in QCD: only A_4 is non-zero.
- At NLO in QCD: A_0 – A_3 also become non-zero
- At NNLO: $A_{5,6,7}$ are expected to become non-zero, while remaining small
 - they arise from gluon loops that are included in the calculations.
 - The Lam–Tung relation predicts $A_0 - A_2 = 0$ is expected to hold up to $O(\alpha_s)$, but can be violated at higher orders.
- A_3 and A_4 depend on the product of vector and axial couplings to quarks and leptons, and are sensitive to the Weinberg angle $\sin 2\theta_W$.**

$$\langle P(\cos\theta, \phi) \rangle = \frac{\int P(\cos\theta, \phi) d\sigma(\cos\theta, \phi) d\cos\theta d\phi}{\int d\sigma(\cos\theta, \phi) d\cos\theta d\phi}$$

$$\langle 1 + \cos^2 \theta \rangle$$

$$\langle \frac{1}{2}(1 - 3\cos^2 \theta) \rangle = \frac{3}{20}(A_0 - \frac{2}{3})$$

$$\langle \sin 2\theta \cos \phi \rangle = \frac{1}{5} A_1$$

$$\langle \sin^2 \theta \cos 2\phi \rangle = \frac{1}{10} A_2$$

$$\langle \sin \theta \cos \phi \rangle = \frac{1}{4} A_3$$

$$\langle \cos \theta \rangle = \frac{1}{4} A_4$$

$$\langle \sin^2 \theta \sin 2\phi \rangle = \frac{1}{5} A_5$$

$$\langle \sin 2\theta \sin \phi \rangle = \frac{1}{5} A_6$$

$$\langle \sin \theta \sin \phi \rangle = \frac{1}{4} A_7$$

Analysis Selection

ATLAS

- Data at $\sqrt{s}=8$ TeV, 20.3 fb⁻¹
- **Measure all A_i (A_0 - A_7)**
- **Measurement performed in 3 independent channels**
 - Muons: central central (CC)
 - Electrons: central central (CC)
 - Electrons: central forward (CF)
- Fiducial volume:
 - CC and $\mu\mu$: $p_T > 25$ GeV, $|\eta| < 2.4$
 - CF: $p_T > 20$ GeV, $2.5 < |\eta| < 4.9$
 - OS dileptons $80 < M_{\parallel} < 100$ GeV
- Backgrounds:
 - EW & $t\bar{t}$ from simulation
 - Multi-jet: data driven
- Binning scheme
 - $|\eta| = [0, 1.0, 2.0, 3.5]$
 - $p_T^Z = [0, 2.5, 5, 8, 11.4, 14.9, 18.5, 22, 25.5, 29, 32.6, 36.4, 40.4, 44.9, 50.2, 56.4, 63.9, 73.4, 85.4, 105, 132, 173, 253, 600]$

CMS

- Data at $\sqrt{s}=8$ TeV, 19.7 fb⁻¹
- **Measure A_0 - A_4**
- **Measurement performed in the muon channel**
- Fiducial volume:
 - $\mu(\mu)$: $p_T > 25(10)$ GeV, $|\eta| < 2.1(2.4)$
 - OS dimuons $81 < M_{\parallel} < 101$ GeV
- Backgrounds:
 - EW & $t\bar{t}$ from data
 - Multi-jet: data driven
- Binning scheme
 - $|\eta| = [0, 1.0, 2.1]$
 - $p_T^Z = [0.0, 10, 20, 35, 55, 80, 120, 200, \text{inf}]$

Methodology

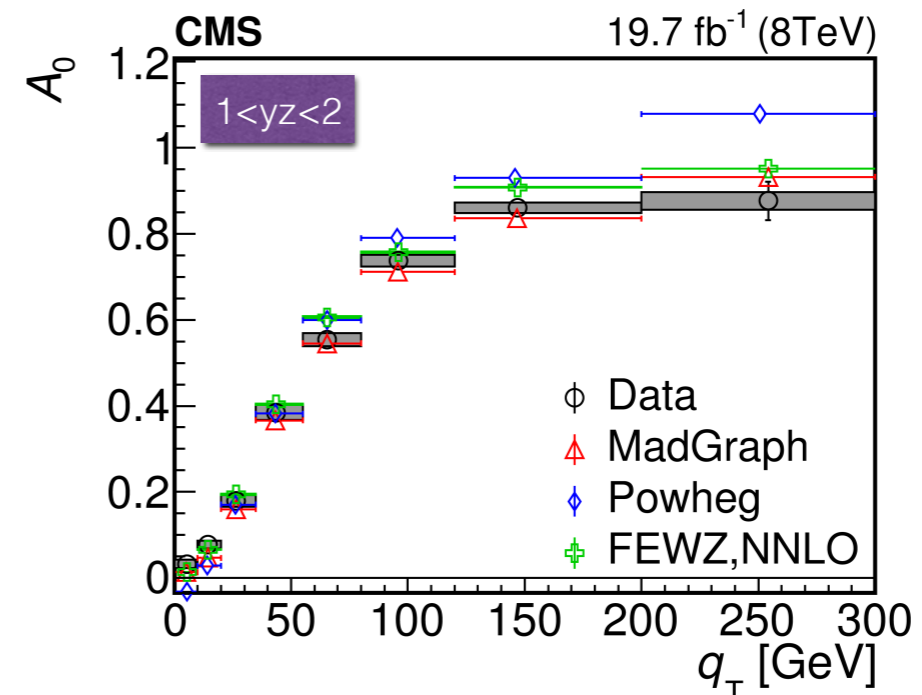
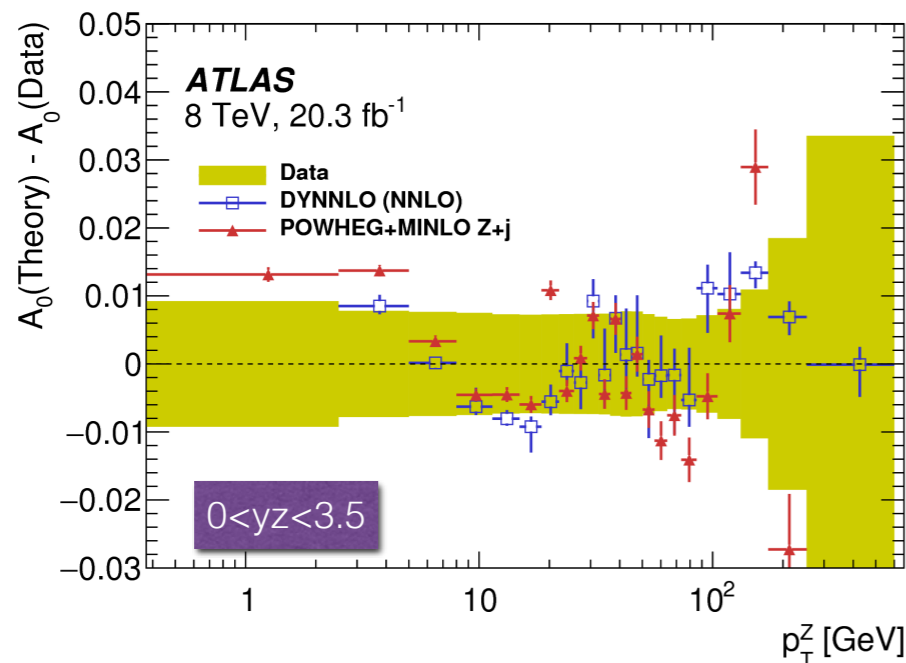
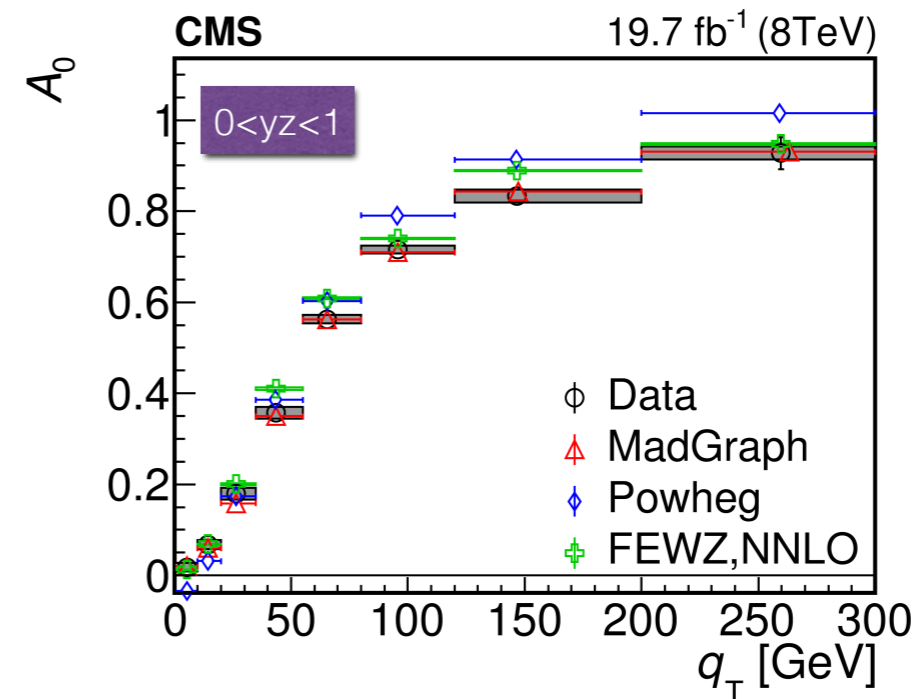
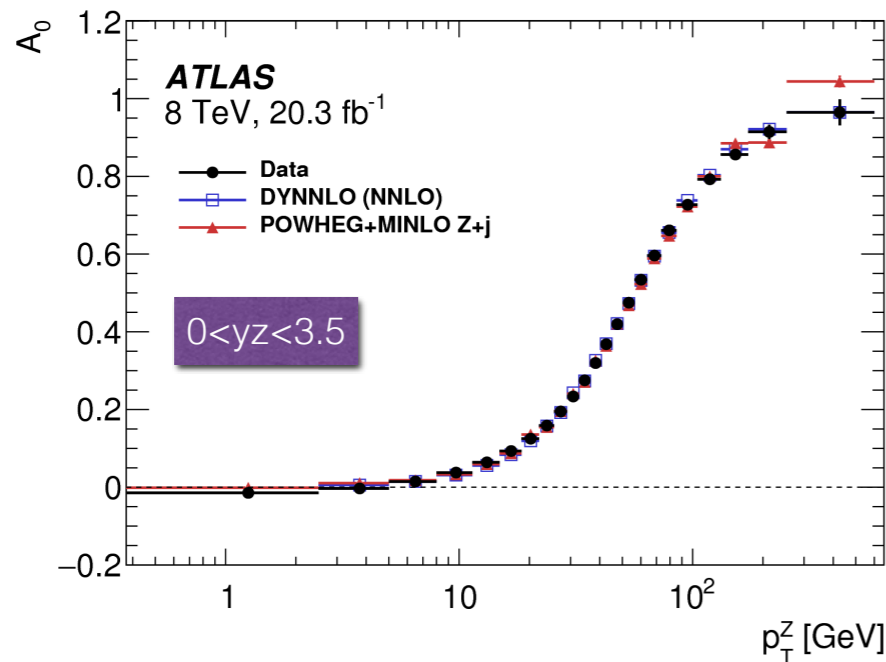
- Similar methodology is applied to both ATLAS and CMS
- The coefficients are extracted from the data by fitting templates of the P_i polynomial terms to the reconstructed angular distributions.
- Each template is normalized by free parameters for its corresponding coefficient A_i , (plus a common parameter for the unpolarized cross-section)
 - Defined independently in each bin of p_T^Z
- A_i extracted from fit
- Fit implemented as maximum likelihood fit
 - Nuisance parameter for each systematic uncertainty
 - Background templates included

Angular distributions sculpted by fiducial acceptance selection

Templates of the P_i terms account for this (MC models the acceptance, efficiency, and migrations)

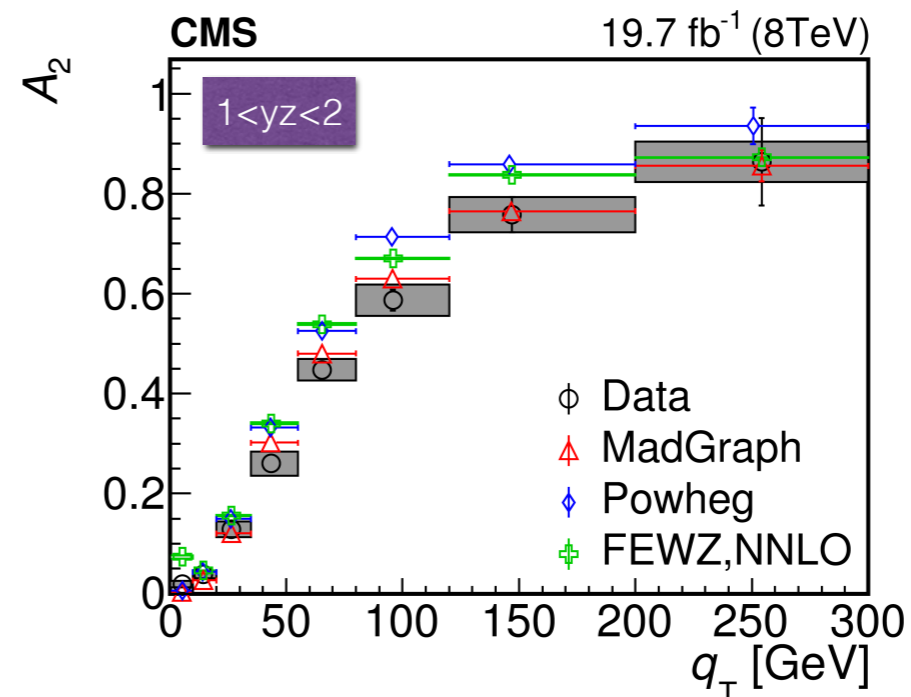
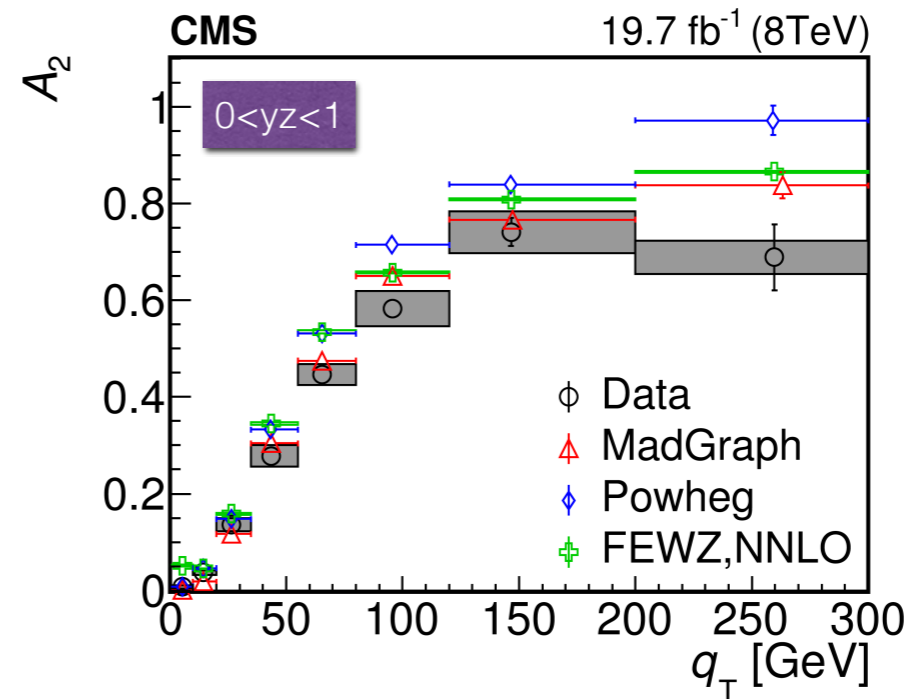
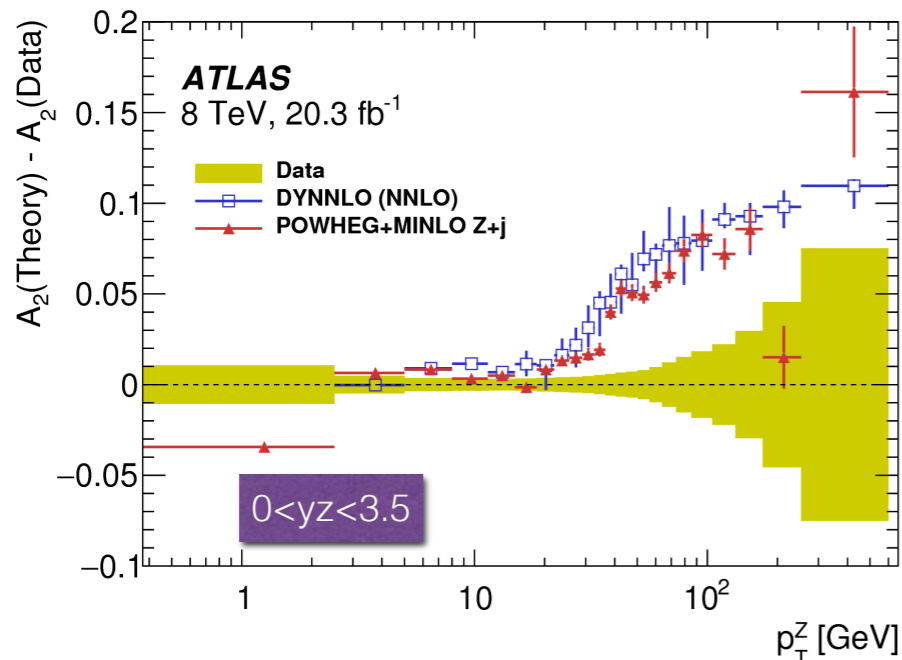
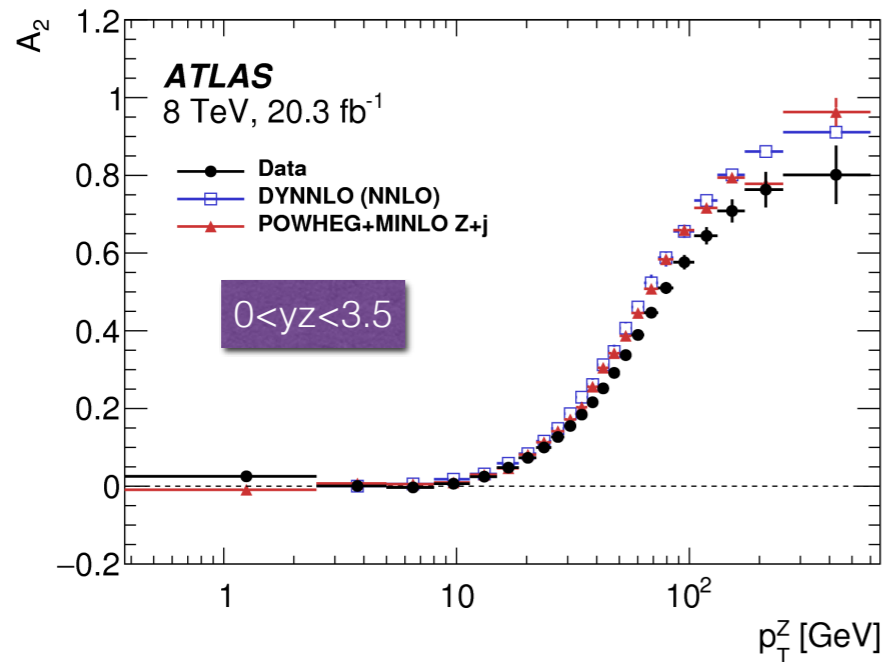
Angular coefficients in Z-boson events, 8 TeV - A_0

- ATLAS: NNLO perturbative QCD predictions (DYNNLO) are in good agreement with the data for A_0
- CMS: Madgraph and FEWZ(NNLO) agree better with data than Powheg(NLO)



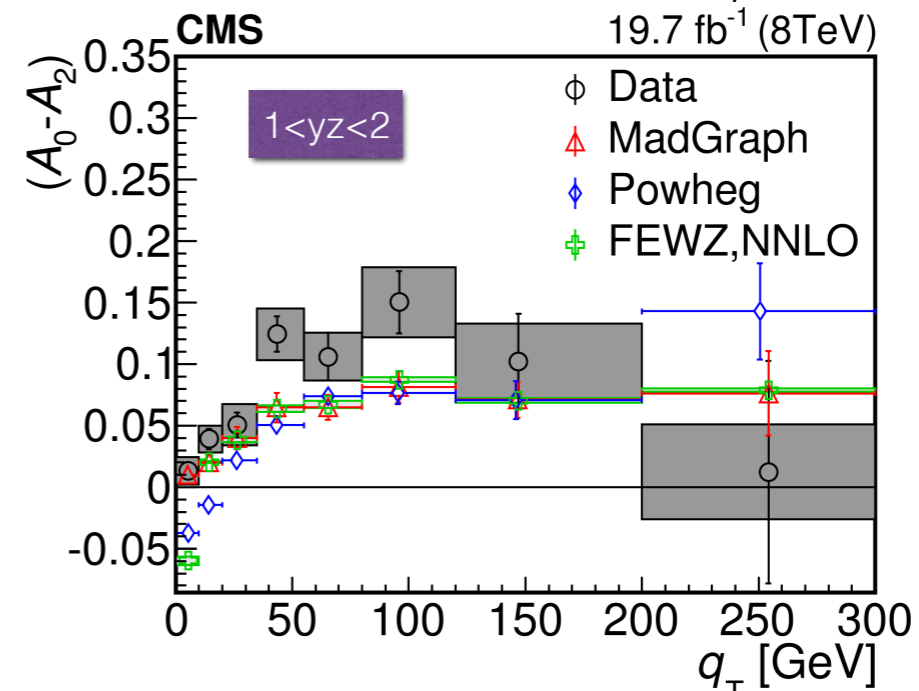
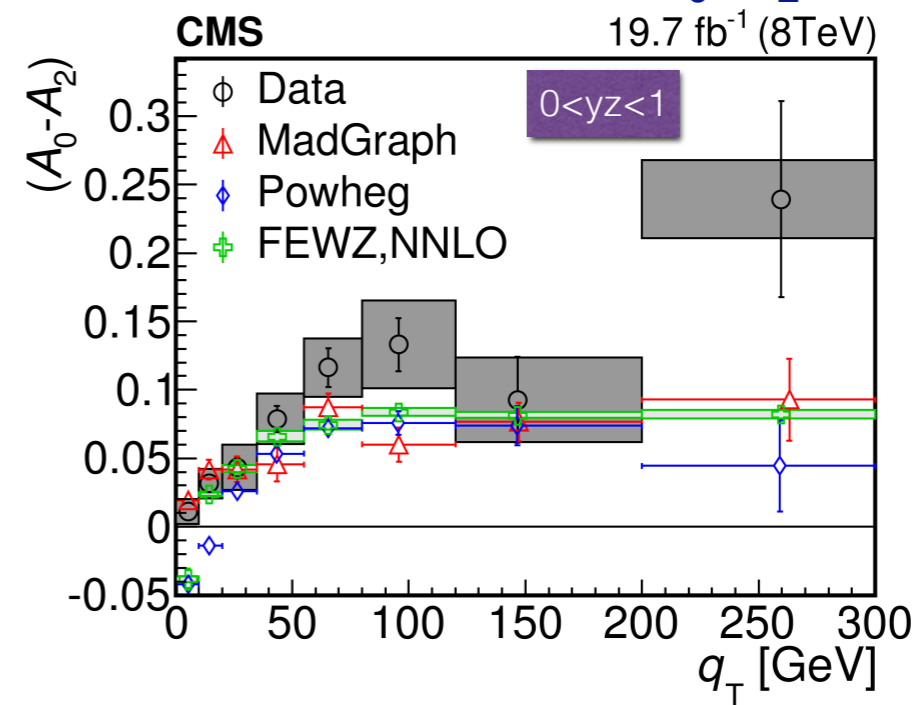
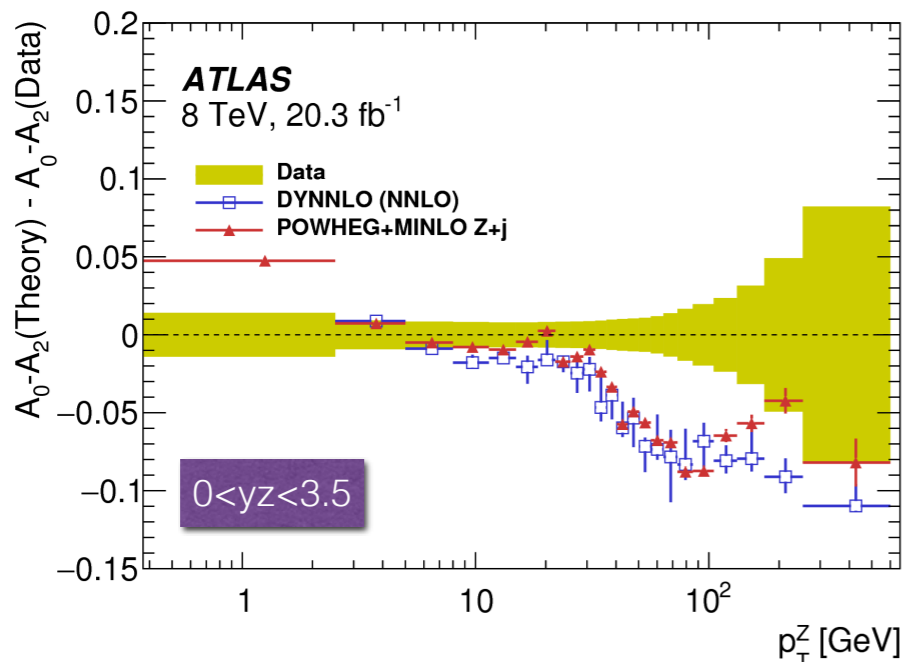
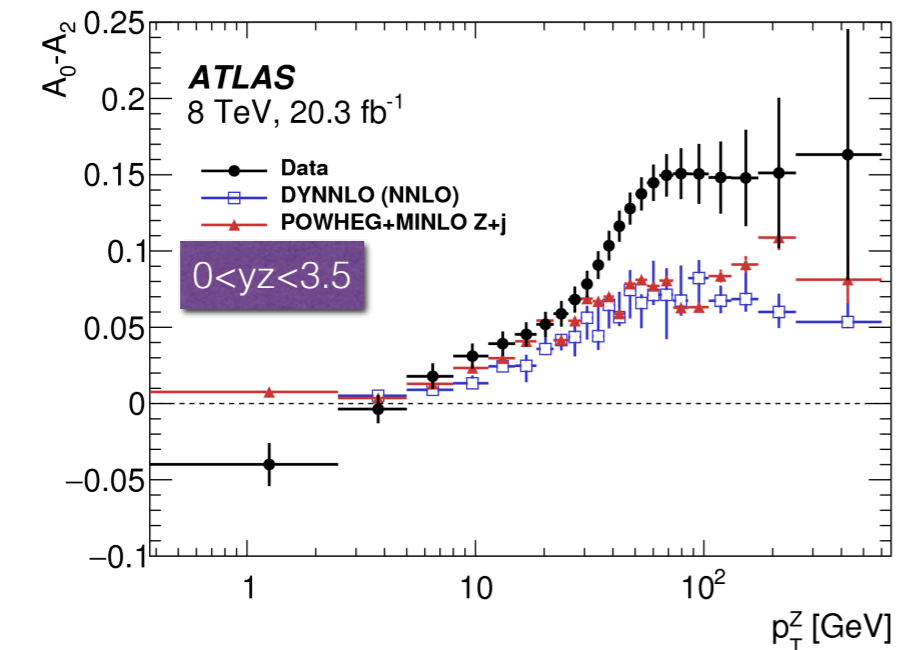
Angular coefficients in Z-boson events, 8 TeV - A_2

- A_2 in data rises more slowly as p_T^Z increases than in the calculations
- Some disagreement at very low and at high p_T between NNLO perturbative QCD predictions and data for A_2



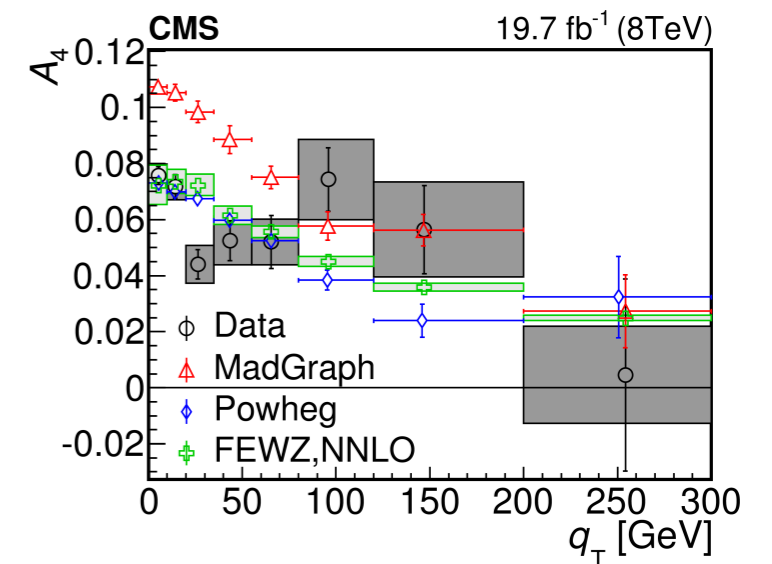
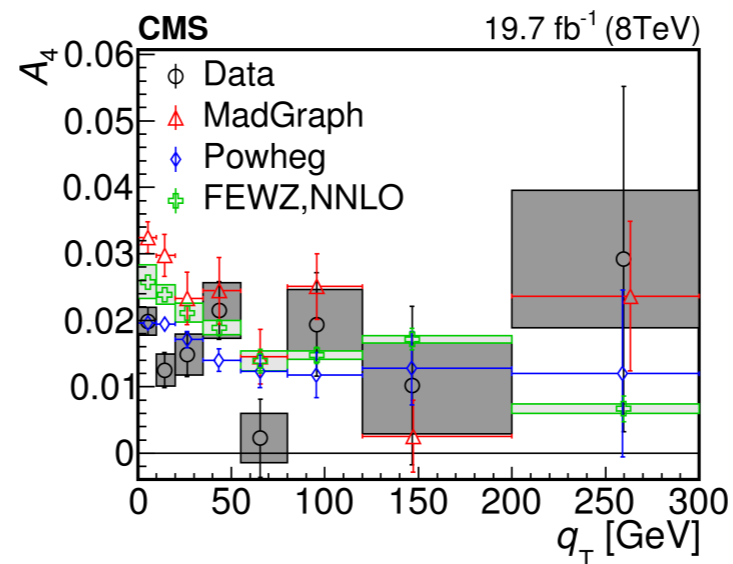
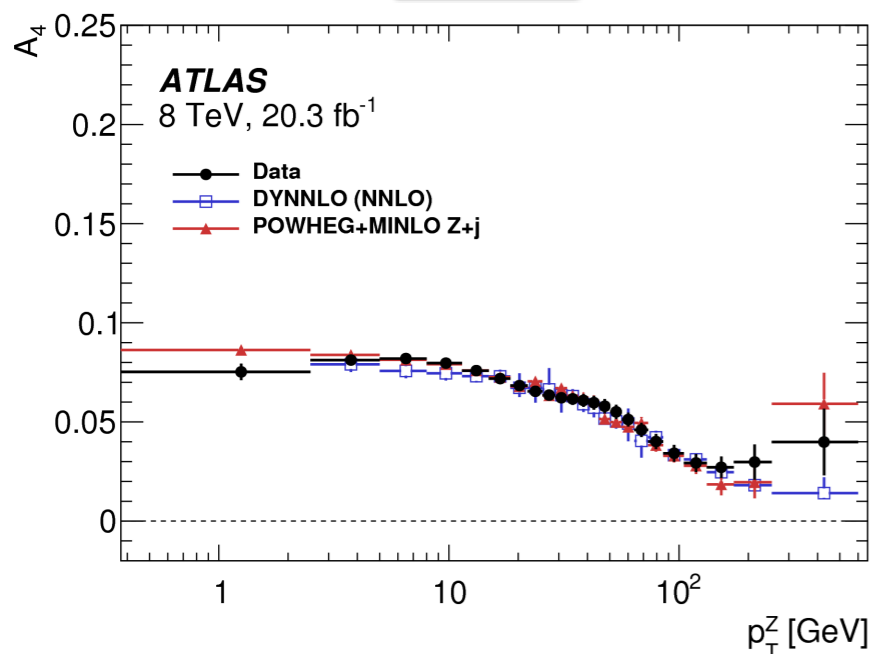
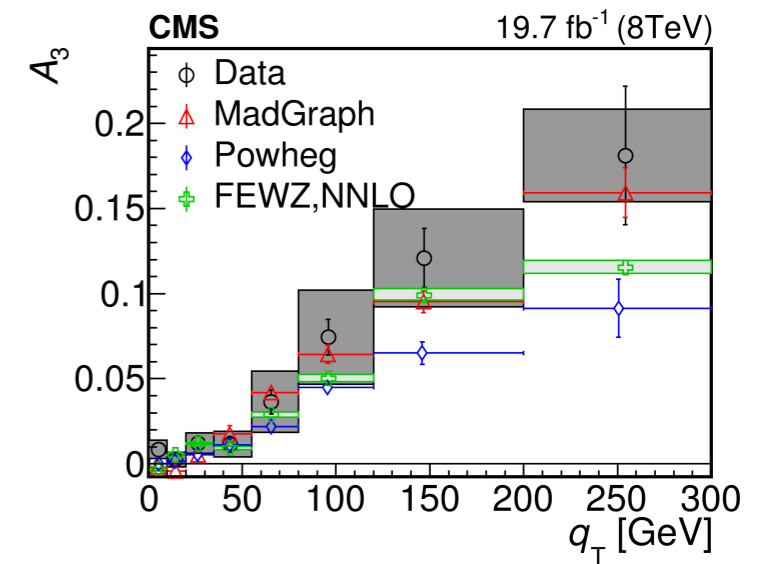
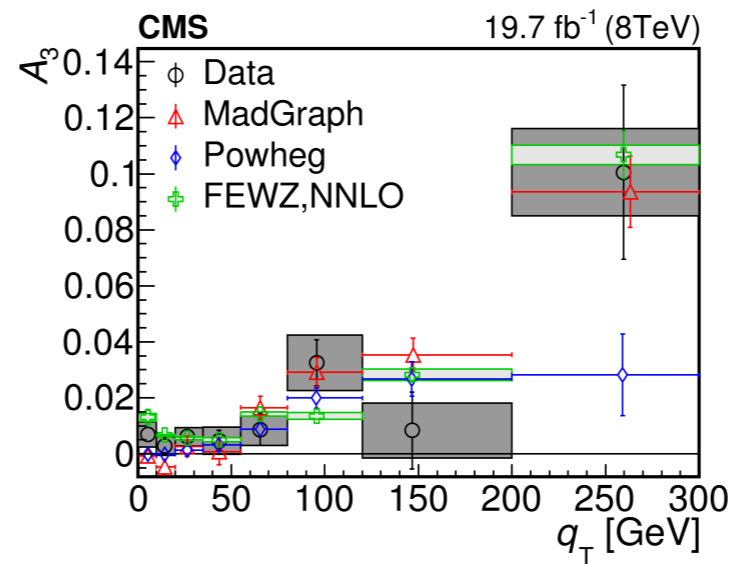
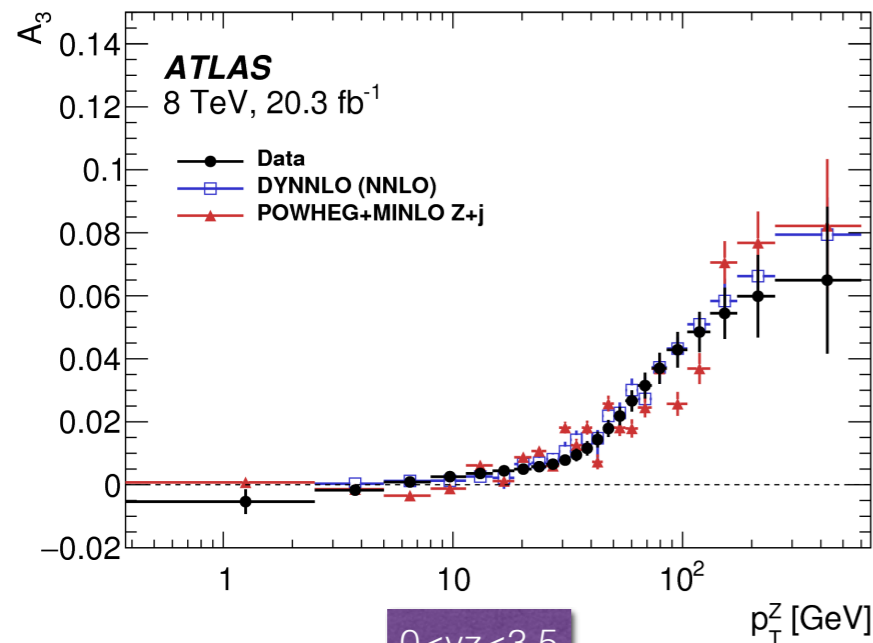
Angular coefficients in Z-boson events, 8 TeV - A_0 - A_2

- Violation of the Lam–Tung relation ($A_0 = A_2$) anticipated by QCD calculations beyond LO
- Significant deviation from NNLO calculations is observed for A_0 - A_2



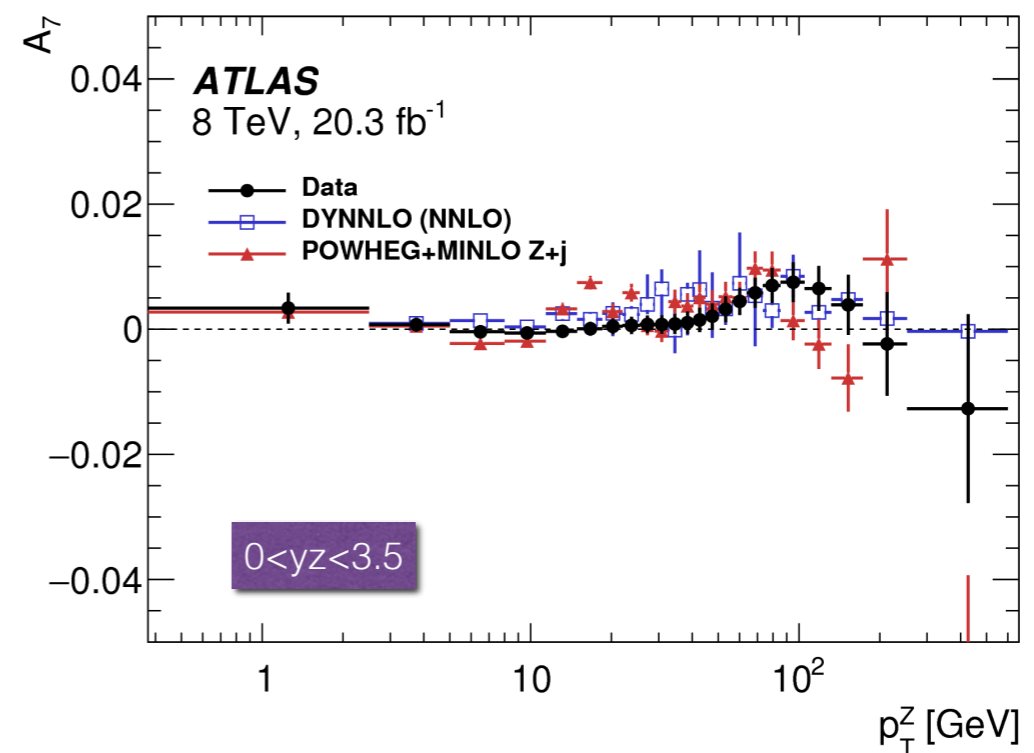
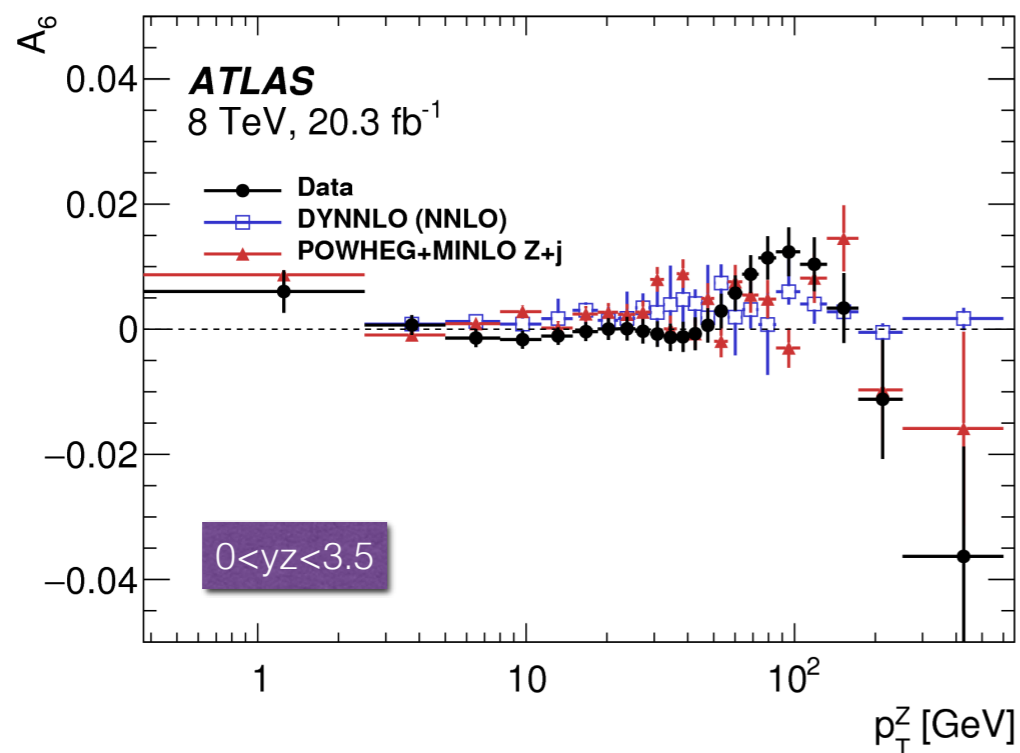
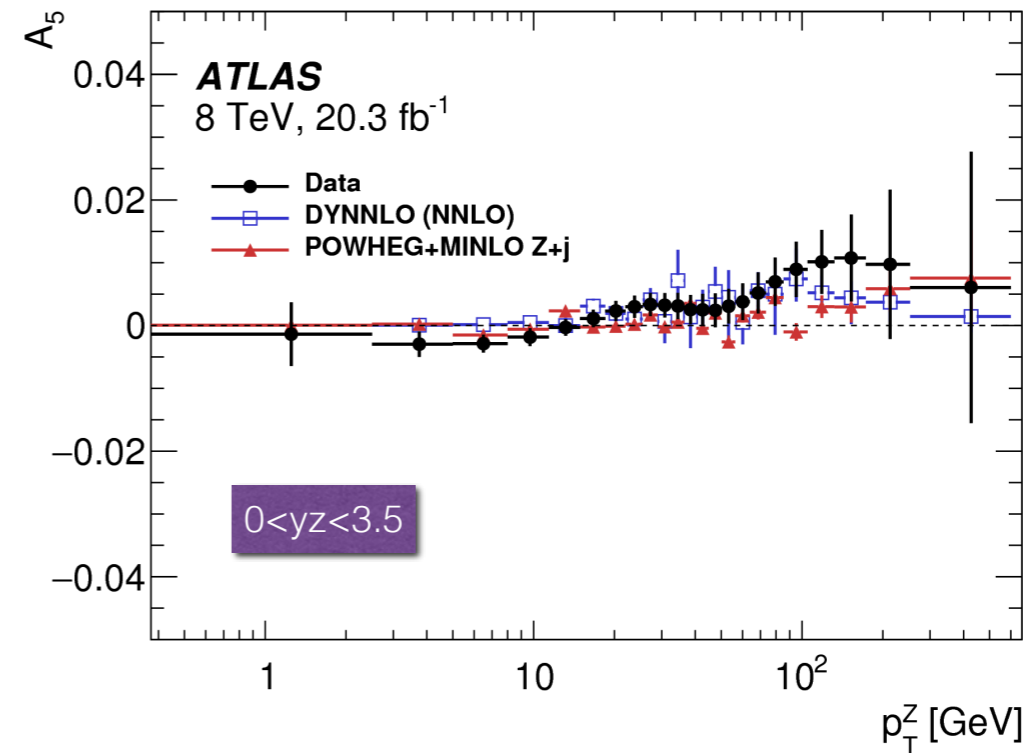
Angular coefficients in Z-boson events, 8 TeV - A_3, A_4

- NNLO perturbative QCD predictions are in good agreement with the data for A_3, A_4



Angular coefficients in Z-boson events, 8 TeV - A_5 , A_6 , A_7

- ATLAS measured the A_5 , A_6 , A_7 coefficients for the first time
- Evidence at the 3σ level is found for non-zero $A_{5,6,7}$ coefficients
 - consistent with expectations from DYNNLO at $O(\alpha^2s)$.



φ^* measurement

φ^* measurement

- Measurements of $p_T^{\ell\ell}$ require a precise understanding of the p_T calibration and resolution of the final-state leptons.
 - Associated systematic uncertainties affect the resolution and limit the ultimate precision of the measurements, particularly at low- p_T
- To minimize the impact of these uncertainties, the φ^* was introduced as an alternative probe of $p_T^{\ell\ell}$

$$\phi_\eta^* = \tan\left(\frac{\pi - \Delta\phi}{2}\right) \cdot \sin(\theta_\eta^*)$$

azimuthal angle in radians
between the two leptons

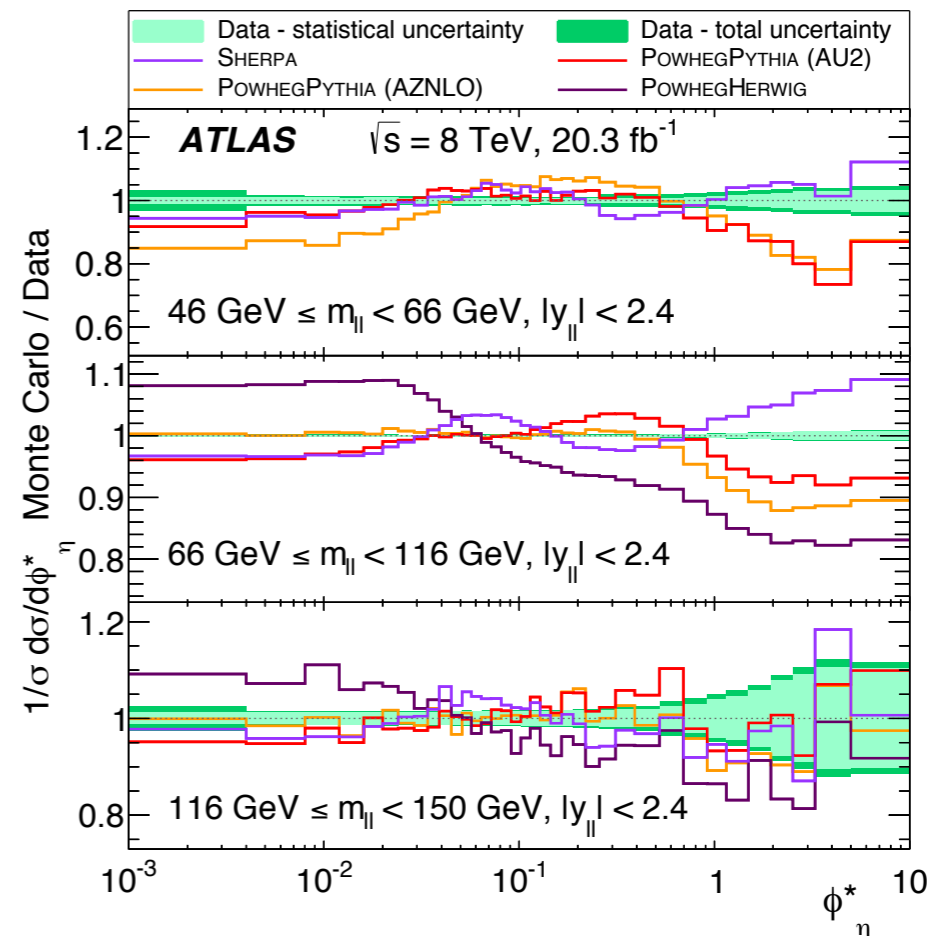
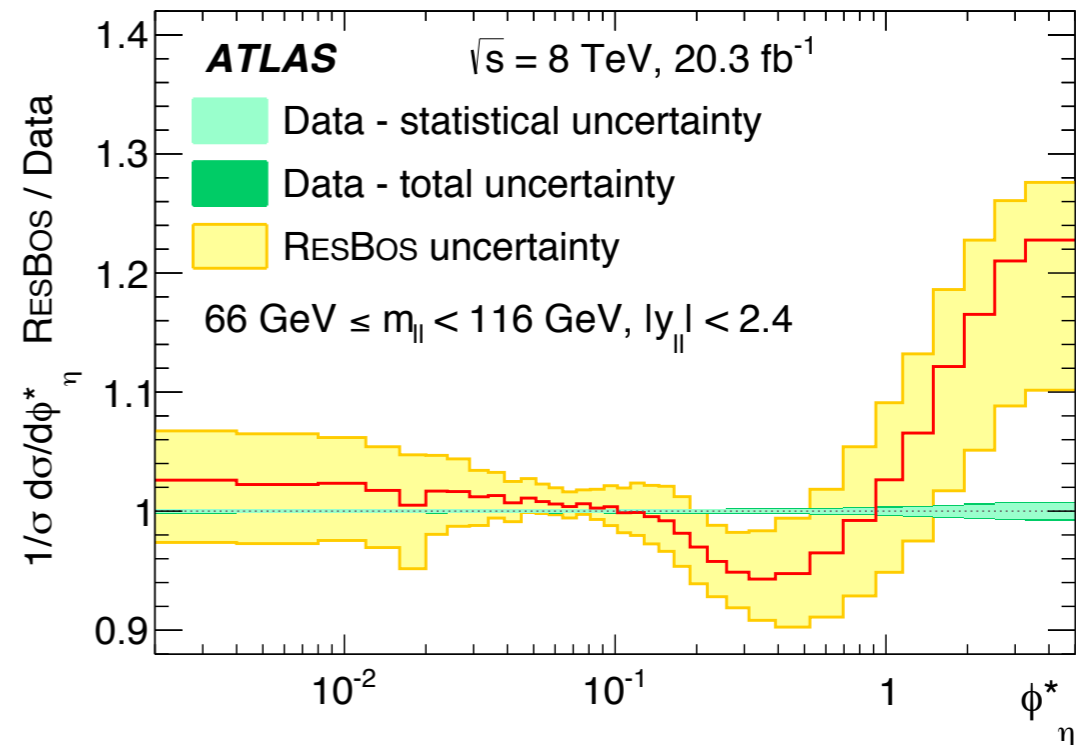
is a measure of the scattering angle of
the leptons with respect to the proton
beam direction in the rest frame of the
dilepton system

$$\cos(\theta_\eta^*) = \tanh[(\eta^- - \eta^+)/2]$$

- φ^* probes the same physics!
 - depends exclusively on angular measurements of the leptons.
 - φ^* is correlated to $p_T^{\ell\ell}/M$
 - Better resolution than p_T in particular for low- p_T values

ϕ^* analysis ATLAS

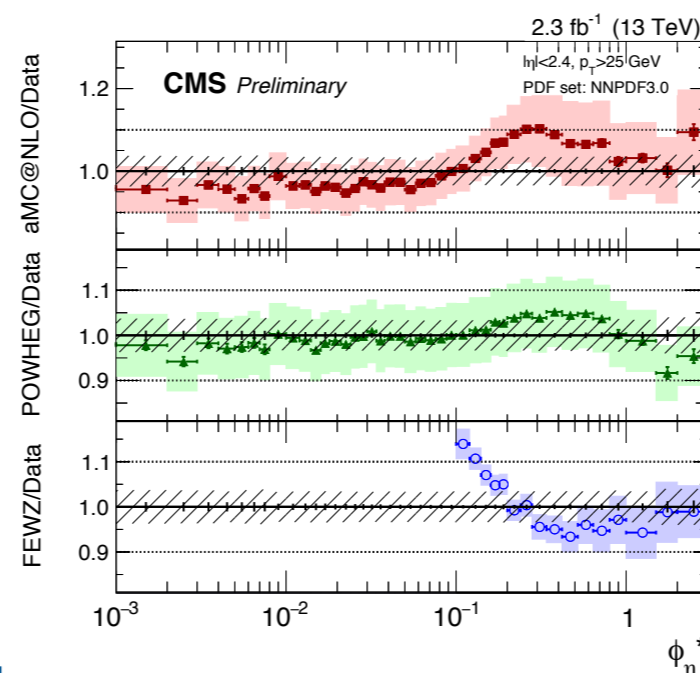
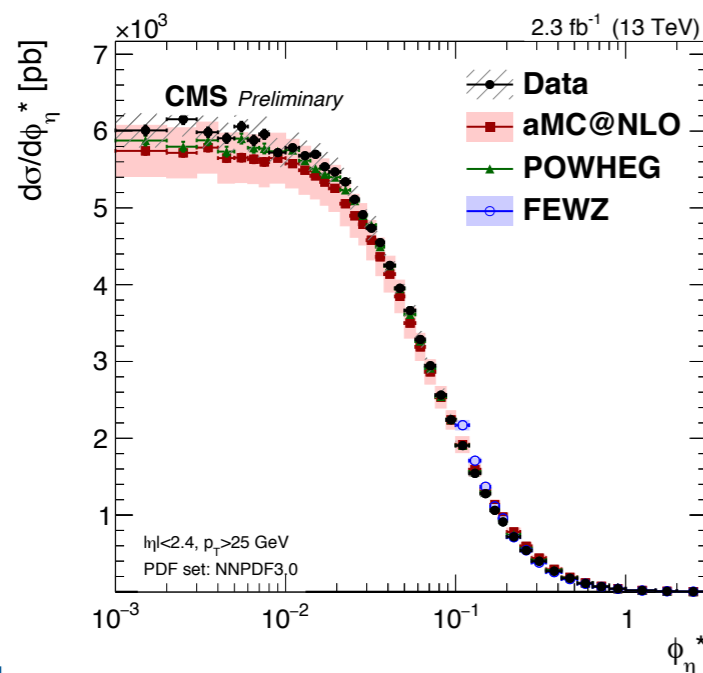
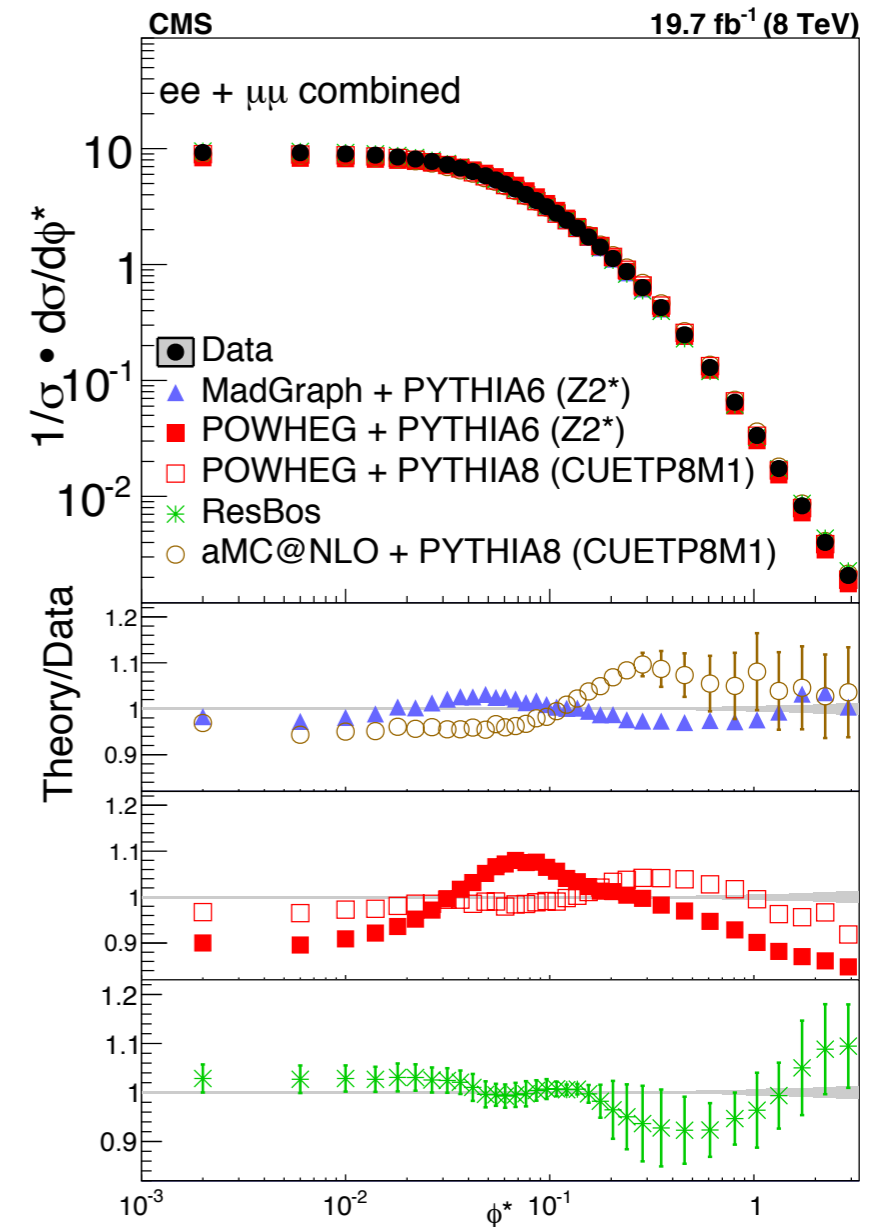
- Low range:
 - Non perturbative effects
 - Soft gluon resummation
 - ResBos predictions agree with data
- High range dominated by :
 - Emission of hard partons
 - ResBos predictions not consistent with data
- Comparison in 3 regions of $M^{\ell\ell}$
 - Up to $\phi^* \sim 2$ MC describe data within $\sim 10\%$
 - Disagreement between simulation & data in peak region
 - Significant disagreement between PowHeg and Sherpa for large ϕ^* values



| | |
|-----------------|---|
| \sqrt{s} | 8 TeV |
| Fiducial Volume | $p_T > 20 \text{ GeV}$ |
| | $ \eta < 2.4$ |
| Backgrounds | $46 < m_{\parallel} < 150 \text{ GeV}$ |
| | Ewk+ttbar from MC Multijet from Data |

φ^* analysis CMS

- At 8 TeV (muon + electron channels):
 - None of the predictions matches the measurements perfectly
 - MADGRAPH+PYTHIA6 provides the best description (Disagreement < 5%)
 - RESBOS, aMC@NLO+PYTHIA8 and POWHEG+PYTHIA8 predictions are also successful at low φ^* but they disagree ~10% for $\varphi^* > 0.1$.
 - POWHEG+PYTHIA6 provides the least accurate prediction, with a disagreement up to 11% for $\varphi^* < 0.1$ and up to 15% for $\varphi^* > 0.1$
- At 13 TeV (muon channel):
 - NNLO prediction from FEWZ gives a good agreement in many regions of the probed phase-space
 - absence of resummation leads to expected deviations at low values of φ^*
 - MADGRAPH5_aMC@NLO and POWHEG show small deviations with a tendency to over predict the distribution, covered by the theory uncertainties

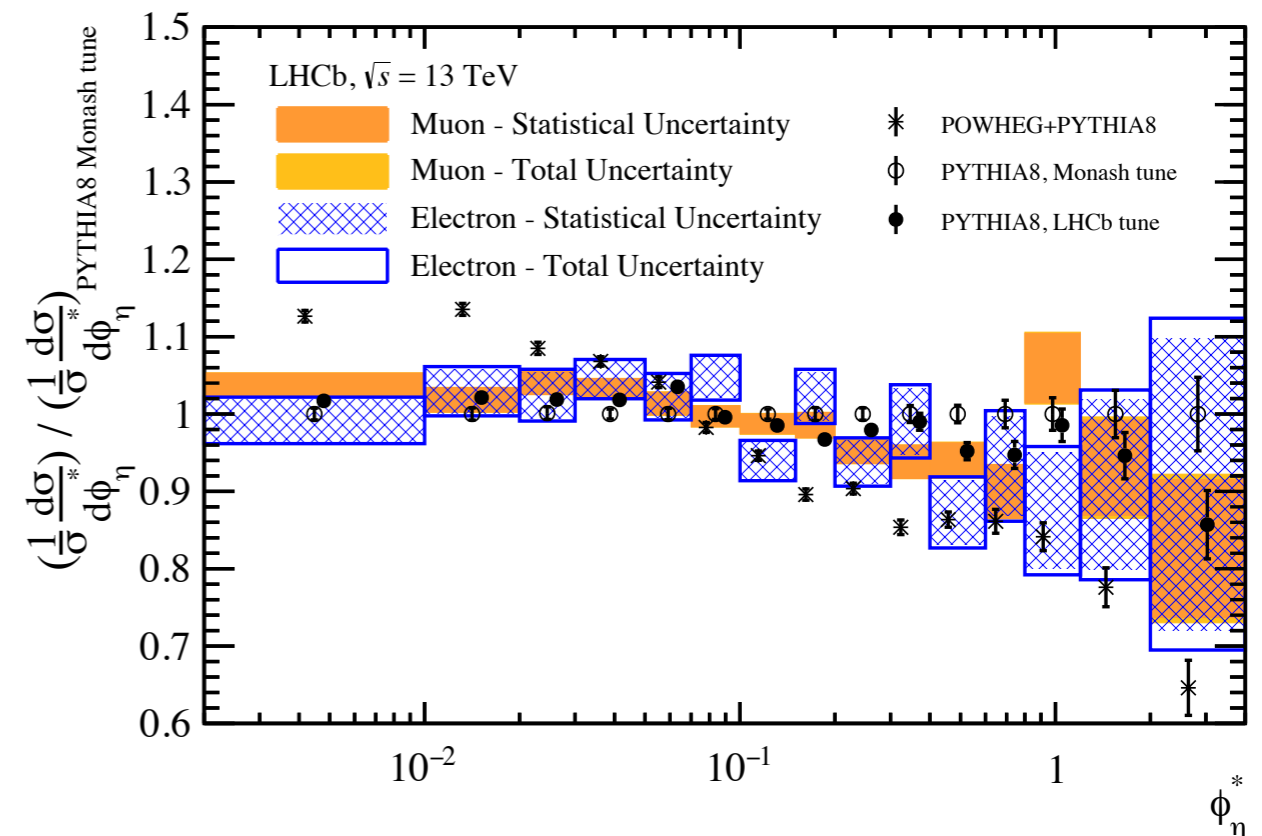
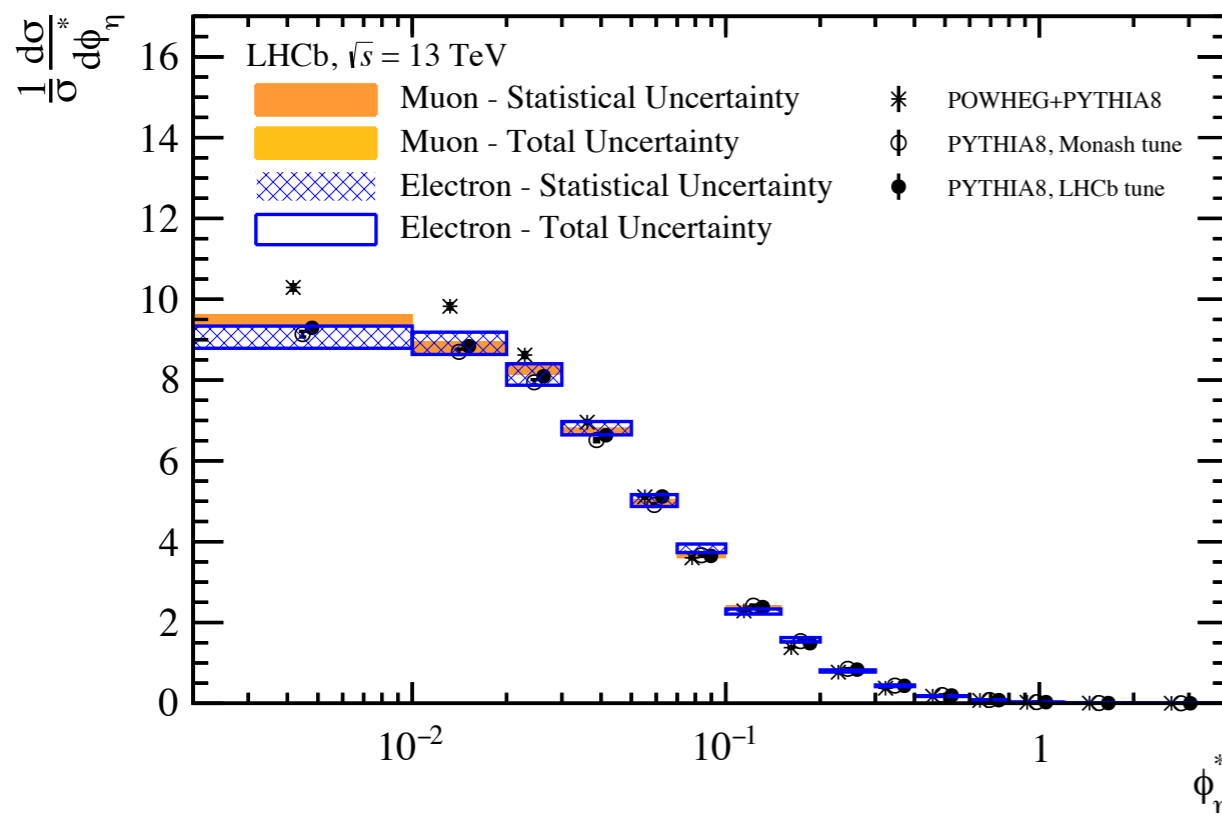


| | |
|-----------------|---|
| \sqrt{s} | 8 TeV, 13 TeV |
| Fiducial Volume | $p_{T1} > 30 \text{ GeV}, p_{T2} > 20 \text{ GeV}$ $ \eta_1 < 2.1 \text{ and } \eta_2 < 2.4$ $60 < m_{ll} < 120 \text{ GeV}$. |
| Backgrounds | Ewk+ttbar from MC Multijet from Data |

φ^* analysis LHCb

- LHCb data agree better with Pythia8 predictions than with Powheg
- Pythia8 with LHCb specific tune of does not describe the data significantly better than the Pythia8+Monash 2013 tune.

| | |
|----------------------------|--------------------------------|
| \sqrt{s} | 13 TeV |
| Int. L (fb ⁻¹) | 294 pb ⁻¹ |
| Fiducial Volume | $p_T > 20\text{GeV}$ |
| | $2.0 < \eta < 4.5$ |
| | $60 < m_{ll} < 120\text{ GeV}$ |



A_{FB} and weak mixing angle measurements

A_{FB} and weak mixing angle at the LHC

- Angular distributions of leptons in DY also useful for A_{FB} and in turn $\sin^2\theta_W^{\text{eff}}$ measurements

- A_{FB} originates from the interference of vector and axial vector coupling

- Differential cross-section at LO:

$$\frac{d\sigma}{d(\cos\theta)} = \frac{4\pi\alpha^2}{3\hat{s}} \left[\frac{3}{8}A(1 + \cos^2\theta) + B \cos\theta \right]$$

θ is the angle of the neg. lepton relative to the quark momentum in the dilepton rest frame

- Linear term** describes the asymmetry in the polar angle θ defined as:

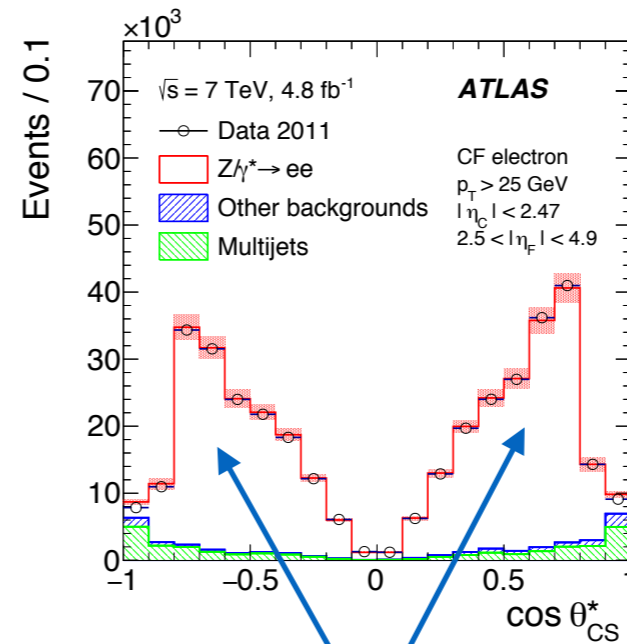
$$A_{FB} = \frac{\sigma_F - \sigma_B}{\sigma_F + \sigma_B} \quad F (B) \text{ denotes } \cos\theta^* > 0 (< 0)$$

θ^* defined in the Collins-Soper frame

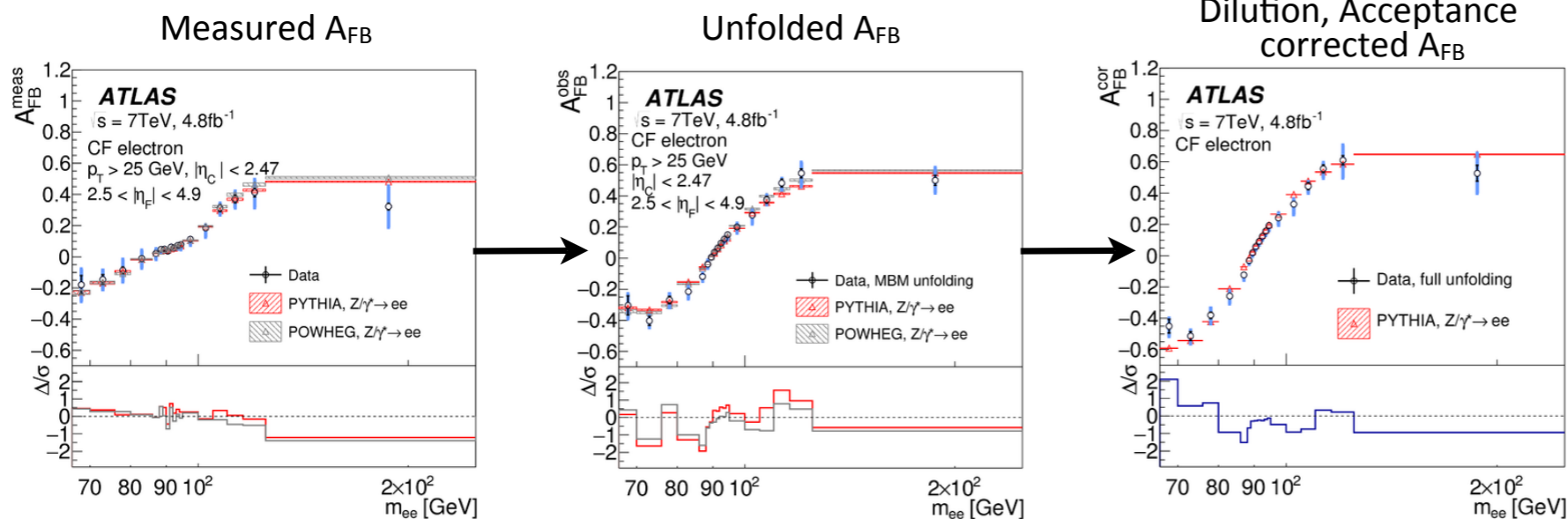
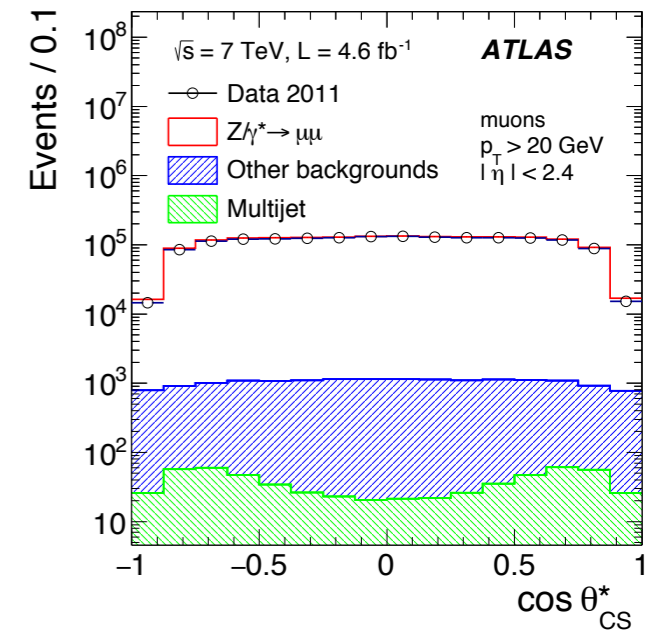
- $A_{FB}(M)$ is sensitive to the electroweak mixing angle, $\sin^2\theta_W$
- A_{FB} has strong dependence on dilepton mass and rapidity
 - A_{FB} is close to zero near M_Z , large and negative at low M_Z , but large and positive at high M_Z
 - More pronounced at large Y_Z due to better identification of q direction...
- ...sensitivity to the weak mixing angle increases at higher Y_Z**

A_{FB} in ATLAS (1/2)

- 7 TeV data, $\int L dt = 4.8$ (4.6) fb⁻¹ for electron (muon) channel
- Electron selection : ET > 25 GeV
 - Central (C) electron ($|\eta| < 2.47$)
 - Forward (F) electron ($2.5 < |\eta| < 4.9$) :
- Muon selection : p_T > 20 GeV and $|\eta| < 2.4$
- Red bands contain all experimental systematic uncertainties
- CC and muon channel measure up to m_{ll} < 1000 GeV. Backgrounds in Z peak region ~ 1%
- CF electron only up to M_{ee} < 250 GeV due to large backgrounds. Backgrounds in Z peak region ~ 5%



For CF electrons in linear scale asymmetry is directly visible on the plot

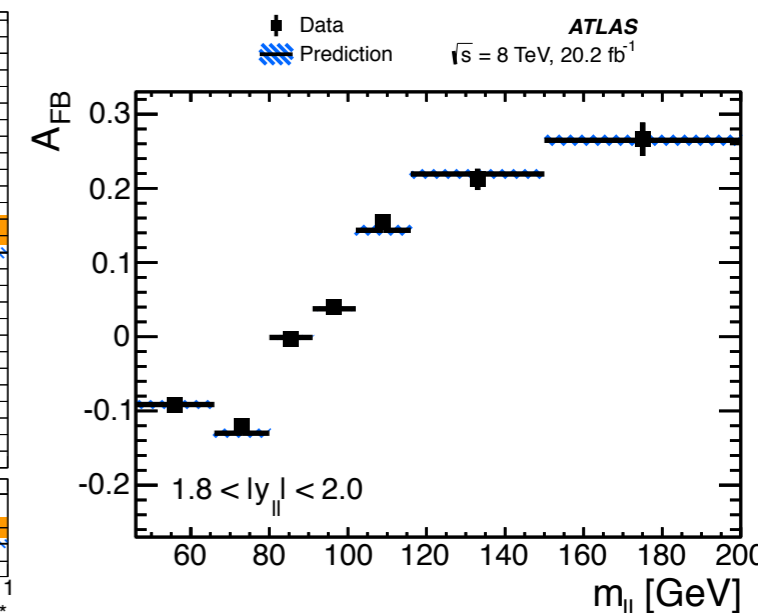
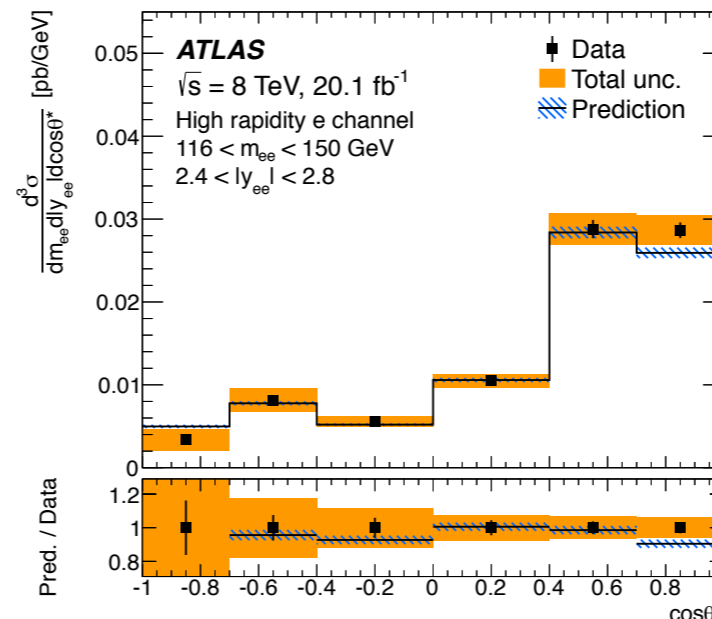
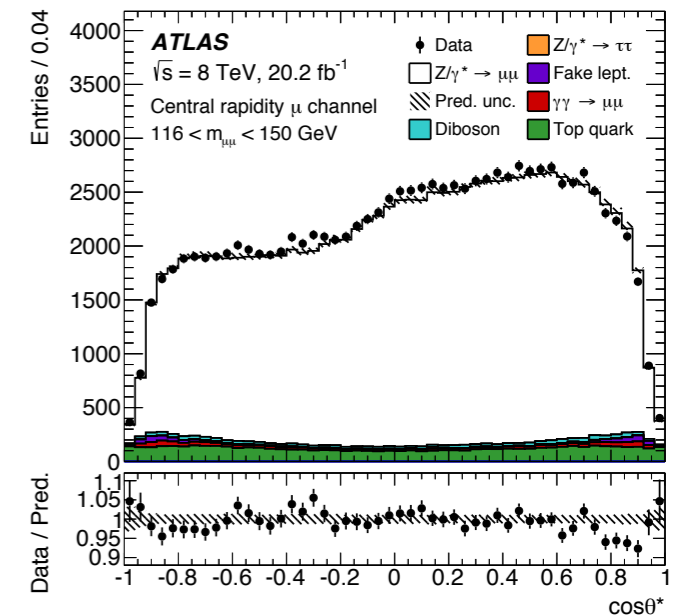
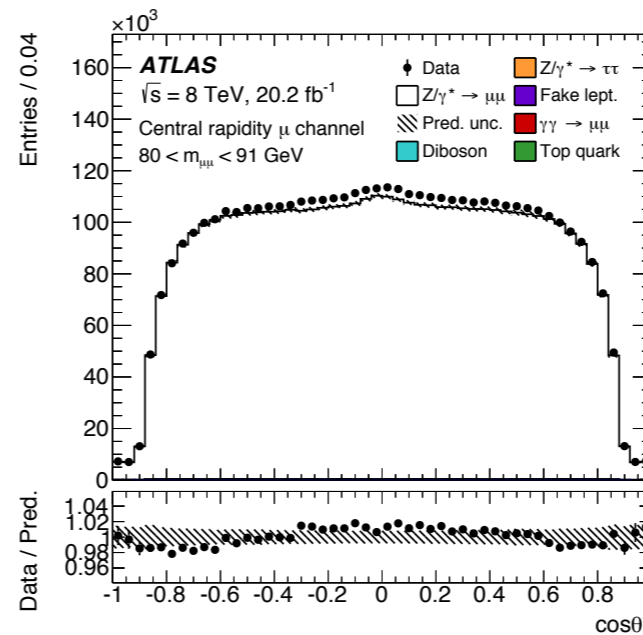


A_{FB} measurement is used to extract the effective weak mixing angle

$$\sin^2 \theta_W^{\text{eff}} = 0.2308 \pm 0.0005(\text{stat}) \pm 0.0006(\text{syst}) \pm 0.0009(\text{PDF})$$

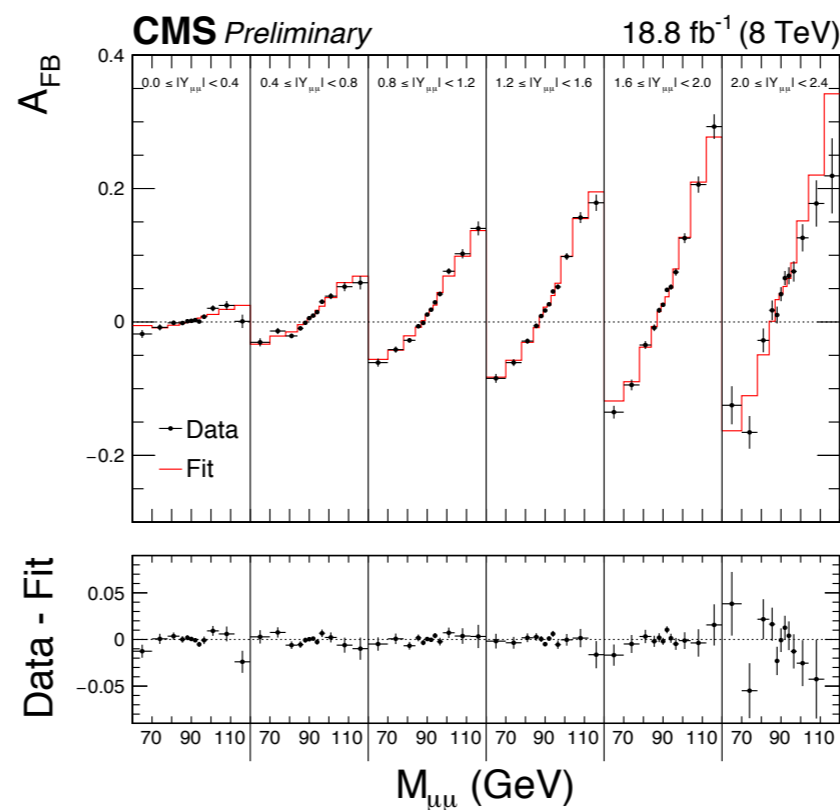
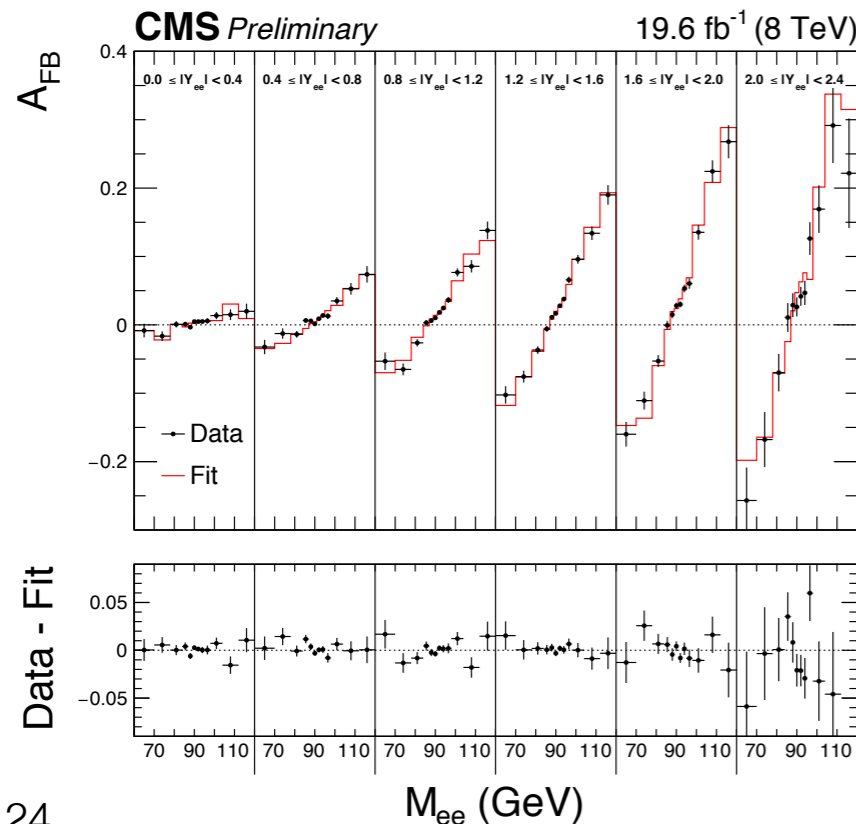
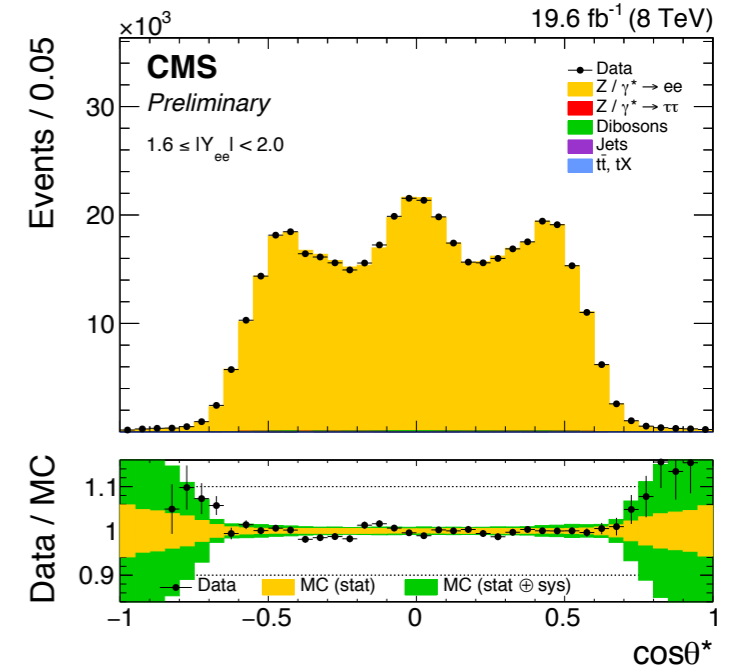
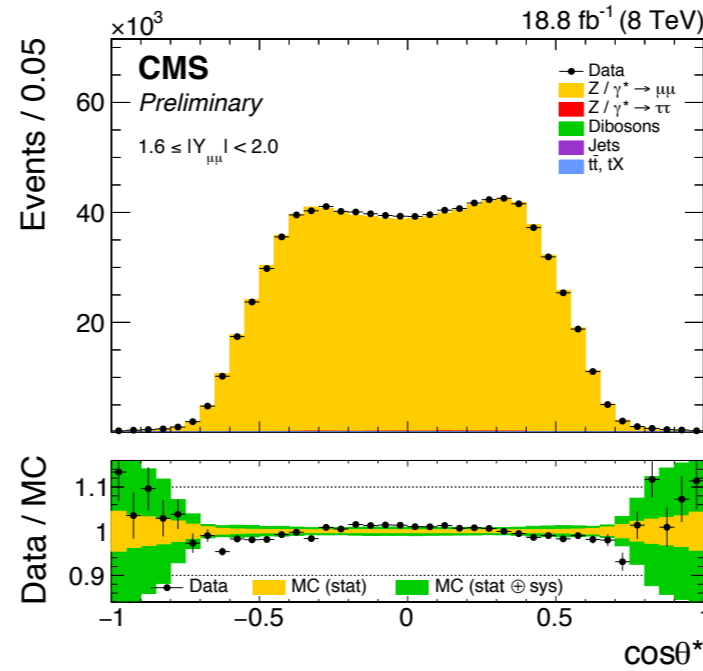
A_{FB} in ATLAS (2/2)

- 8 TeV data, $\int L dt = 20.2 \text{ fb}^{-1}$, measurement in the context of the Triple differential cross-section measurement
- Channels and binning:
 - central $|\eta| < 2.4$, $p_T > 20 \text{ GeV}$ electrons and muons,
 - seven $46 < M^{\ell\ell} < 200 \text{ GeV}$, twelve $y_{ll} < 2.4$ and six $\cos\theta_{CS}$ bins
 - one central (with p_T cut increased to 25 GeV) and one forward electron $|\eta| > 2.5$, $p_T > 20 \text{ GeV}$
 - in five $66 < M^{\ell\ell} < 150$, five $1.2 < y_{ll} < 3.6$ and six $\cos\theta_{CS}$ bins
- Prediction from Powheg including NNLO QCD and NLO Ewk K-factors
- A_{FB} in good agreement with predictions
- The total uncertainty is dominated by the data statistical uncertainty everywhere



A_{FB} in CMS

- 8 TeV data, $\int L dt = 19.6$ (18.8) fb⁻¹ for electron (muon) channel
 - Electron selection: $E_T > 30$ and 20 GeV
 - Muon selection : $p_T > 25$ GeV and 15 GeV $| \eta | < 2.4$
 - $60 \text{ GeV} < M_{ll} < 120 \text{ GeV}$
- Measurement in 12 bins of M_{ll} and 6 bins of $| Y_{ll} |$ up to 2.4
- $\sin^2 \theta_W^{\text{eff}}$ extracted from simulation samples generated with different values of $\sin^2 \theta_W^{\text{eff}}$ are compared with the measured A_{FB} , using χ^2

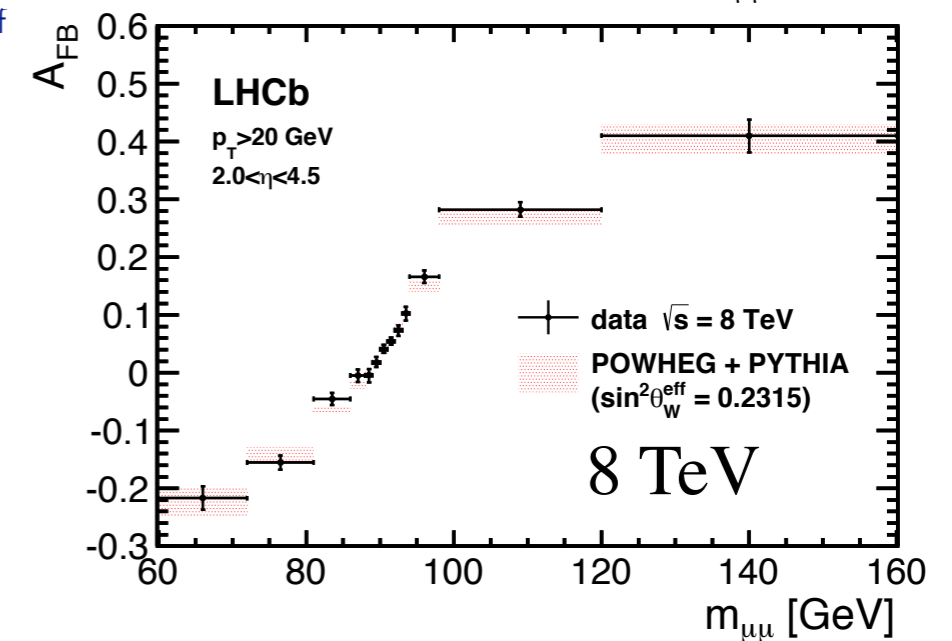
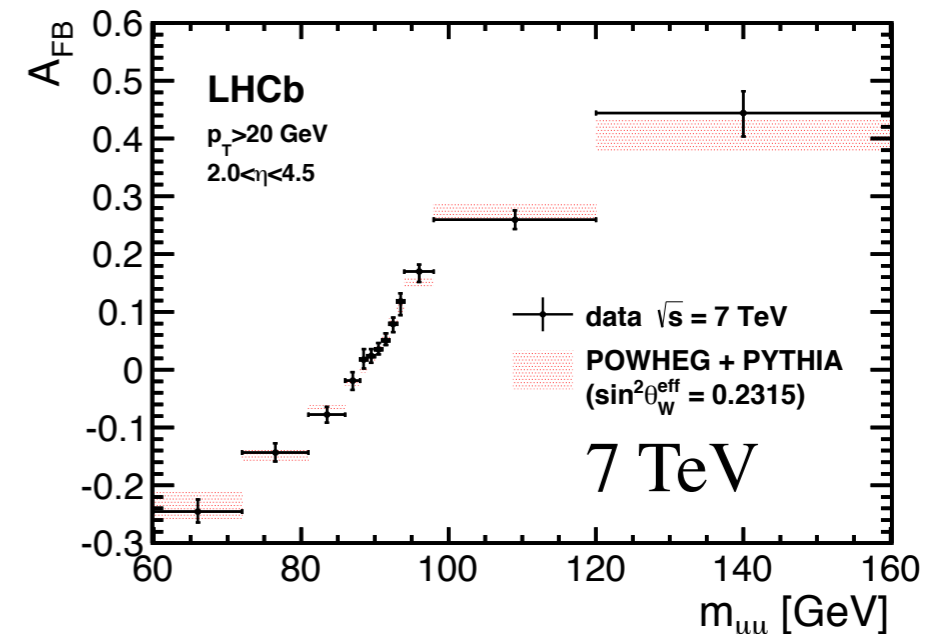
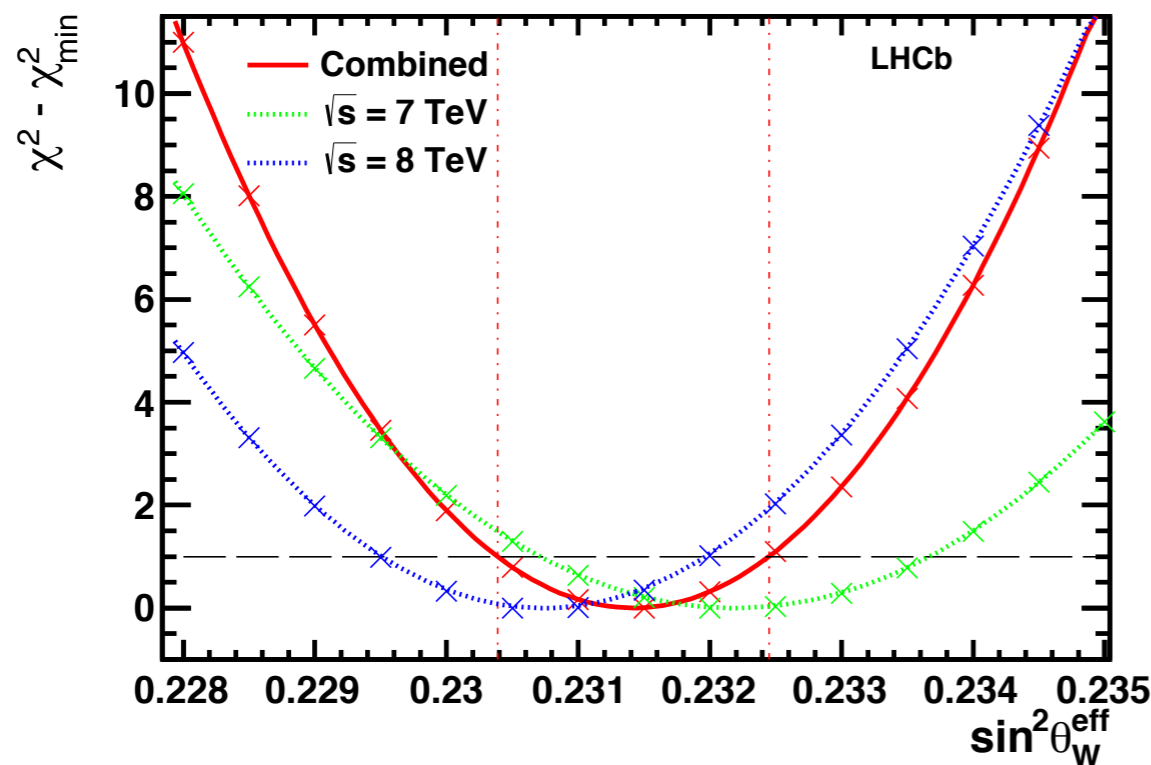


A_{FB} measurement is used to extract the effective weak mixing angle

$$\sin^2 \theta_W^{\text{eff}} = 0.23101 \pm 0.00036(\text{stat}) \pm 0.00018(\text{syst}) \pm 0.00016(\text{theory}) \pm 0.00030(\text{PDF})$$

A_{FB} in LHCb

- 7 and 8 TeV data with $\int Ldt = 1$ and 2 fb^{-1} respectively
- Muon channel only:
 - $2.0 < \eta < 4.5, p_T > 20 \text{ GeV}$
 - invariant mass within $60 < m_{\mu\mu} < 160 \text{ GeV}$.
- The true asymmetry A_{FB} is obtained from the measured A_{FB} through unfolding
- Systematic error dominated by curvature/momentum (PDFs uncertainties for $\sin^2\theta_W^{\text{eff}}$)
- Simulation samples generated with different values of $\sin^2\theta_W^{\text{eff}}$
- Compare simulations with measured A_{FB} , using χ^2



$$\sin^2\theta_W^{\text{eff}} = 0.23142 \pm \underbrace{0.00073}_{\text{stat}} \pm \underbrace{0.00052}_{\text{syst}} \pm \underbrace{0.00056}_{\text{theory}}$$

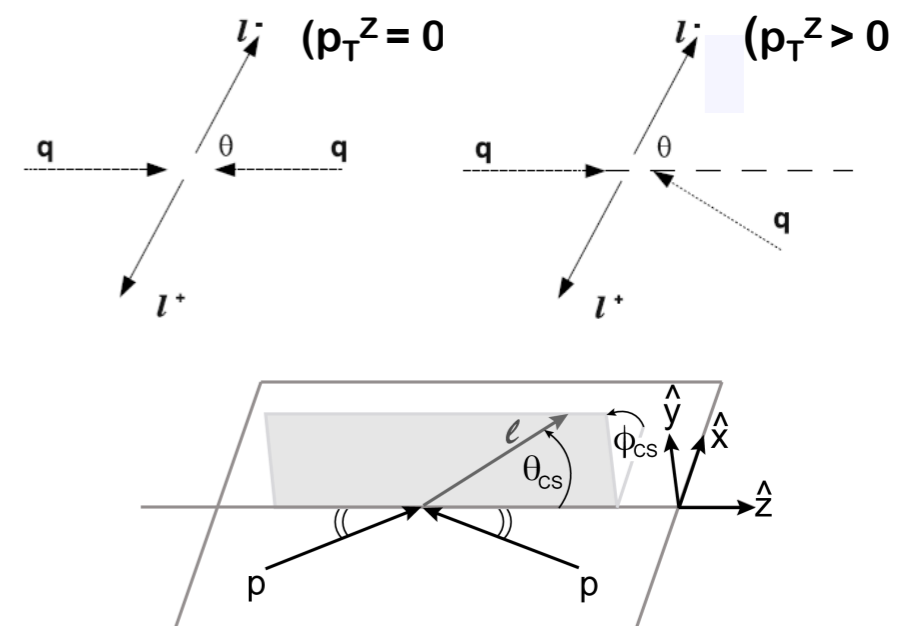
Summary

- After 47 years, the DY process is still an important measurement, which allows
 - fundamental tests of the SM
 - precise determination of QCD and EW parameters
 - searching for new physics
- ATLAS, CMS and LHCb have an extensive and complementary program of DY measurements
- DY measurements will benefit from the large data sample which is being collected in Run 2
 - Larger statistic will allow exploring new corners of the phase space
 - Reduce the systematic uncertainties related to the calibration of the detector

Backup slides

Lepton angular distributions and A_{FB}

- Ambiguity in the definition of the θ angle (and $\cos\theta^*$ sign) when $p_T^{\ell\ell} > 0$ in the Lab.Frame
 - In pp collision, the quark and anti-quark directions are not known
 - q carries more momentum than qbar as qbar must originate from the parton sea
 - On average, Z boson is boosted into the q direction
- The Collins-Soper frame resolves this ambiguity by using a symmetric axis with respect to the incoming partons
- The quark direction (positive z-axis) is determined based on the rapidity direction of the dilepton system in the laboratory frame
 - This assumption leads to a fraction of events with wrongly assigned quark direction, which causes a **dilution** of the observed asymmetry



$$\cos\theta_{CS}^* = \frac{p_{z,\ell\ell}}{|p_{z,\ell\ell}|} \frac{2(p_1^+ p_2^- - p_1^- p_2^+)}{m_{\ell\ell} \sqrt{m_{\ell\ell}^2 + p_{T,\ell\ell}^2}}$$

with $p_i^\pm = \frac{1}{\sqrt{2}}(E_i \pm p_{z,i})$

θ^* is the angle between the lepton momentum and the axis that bisects the direction of one proton and the direction opposite to the other proton in the c.m. frame of the dileptons

Angular coefficients

MC generators - ATLAS

- DYNNLO (v1.3): Inclusive fixed-order pQCD predictions at NNLO for $p_{\text{ZT}} > 2.5 \text{ GeV}$
 - leading order in EW, using the G_{μ} scheme
- The Powheg + MiNLO only including statistical uncertainties obtained using the Z + jet process at NLO
 - The formal accuracy of both calculations is $O(\alpha_s)$ for the predictions of the A_i as a function of p_{ZT} .
- Agreement between the two programs and the data within uncertainties for most coefficients.

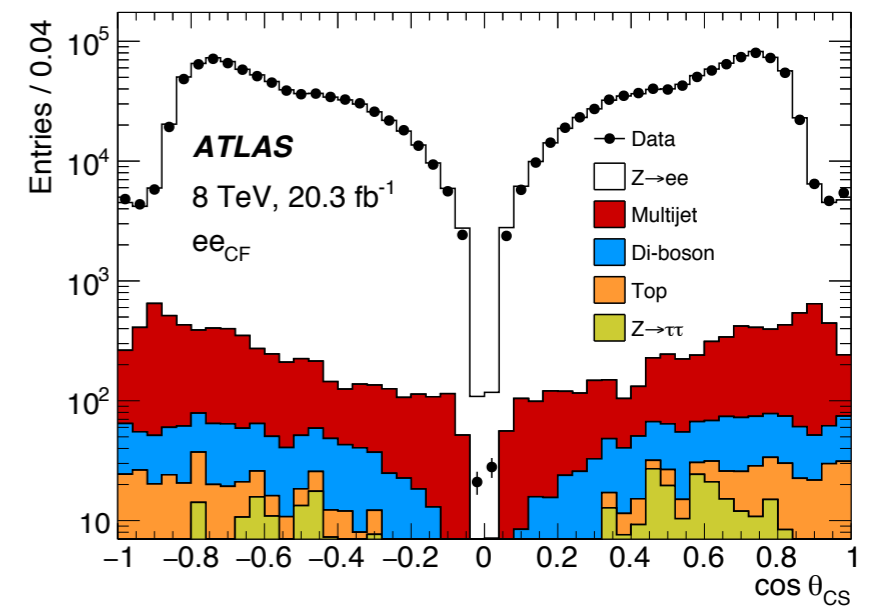
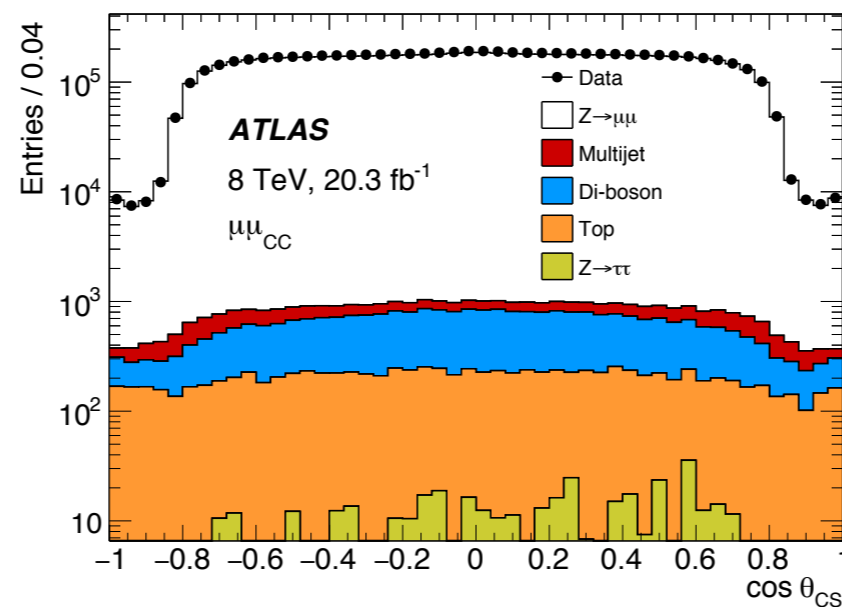
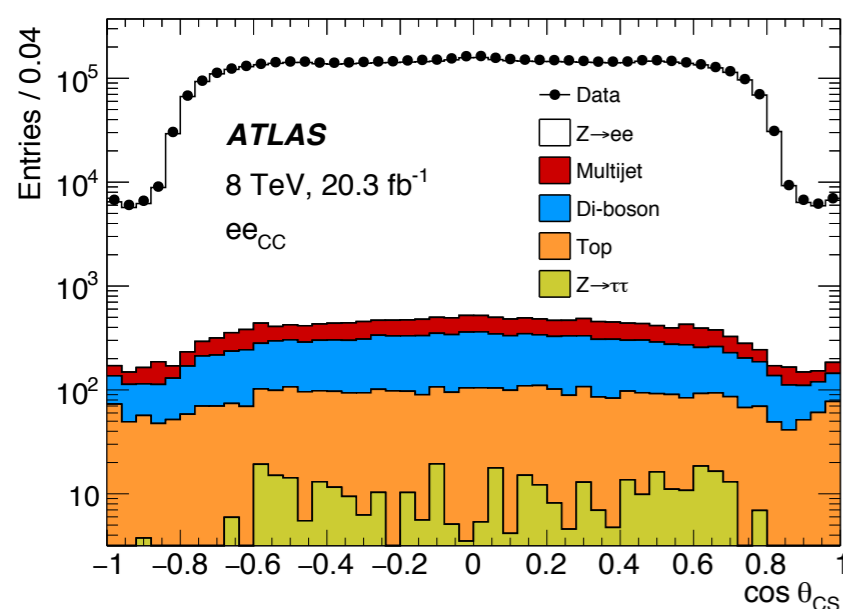
| Signature | Generator | PDF | Parton Sh + Hadr. | FSR | Comments |
|--|--------------------------|-----------------|-------------------|--------|---|
| $Z/\gamma^* \rightarrow \ell\ell$ | POWHEGBOX + PYTHIA 8 | CT10 NLO | AU2 | PHOTOS | Used to test the dependence on different matrix-element calculations and parton-shower models |
| $Z/\gamma^* \rightarrow \ell\ell$ | POWHEGBOX + JIMMY/HERWIG | CT10 NLO | Herwig | PHOTOS | |
| $Z/\gamma^* \rightarrow \ell\ell$ | SHERPA | CT10 NLO | SHERPA | | |
| $Z/\gamma^* \rightarrow \ell\ell + \text{jet}$ | POWHEG + MiNLO | CT10 NLO | | | |
| $W \rightarrow \ell\nu$ | POWHEGBOX + PYTHIA 8 | CT10 NLO | | | |
| $W \rightarrow \ell\nu$ | SHERPA | CT10 NLO | | | |
| $t\bar{t}$ pair | MC@NLO + JIMMY/HERWIG | CT10 NLO | | | |
| Single top quark: t channel | ACERMC + PYTHIA 6 | CTEQ6L1 | | | |
| s and Wt channels | MC@NLO + JIMMY/HERWIG | CT10 NLO | | | |
| Dibosons | SHERPA | CT10 NLO | | | |
| Dibosons | HERWIG | CTEQ6L1 | | | |
| $\gamma\gamma \rightarrow \ell\ell$ | PYTHIA 8 | MRST2004QED NLO | | | |

MC generators - CMS

- The coefficients, measured as a function of q_T and $|\eta|$, are compared with three perturbative QCD predictions
 - FEWZ at NNLO
 - POWHEG at NLO
 - MADGRAPH at LO
- Signal simulated with MADGRAPH with zero to four additional jets, interfaced with PYTHIAv6 with the Z2* tune
 - The CTEQ6L1 PDFs are used
- Multiple-parton interactions are simulated by PYTHIA.
- The POWHEG generator interfaced with PYTHIAv6 and the CT10 PDF set are used as an alternate to test any model dependence in the shapes of the angular distributions.
- Background simulations are performed with MADGRAPH (W +jets, $t\bar{t}$, $\tau\tau$), POWHEG (single top quark), and PYTHIA (WW , WZ , ZZ).
- The normalizations of the inclusive Drell–Yan, W boson, and $t\bar{t}$ distributions are set using NNLO cross sections.

Background composition - ATLAS

- Total background in cc events below 0.5%
 - uncertainty dominated by the large uncertainty in multijet background of $\sim 50\%$
 - uncertainty in the top+ewk taken conservatively to be 20%
- Total background in cf events at the level of 2%
- Non fiducial backgrounds (migrations due to finite resolutions) contribute more in the cf topology

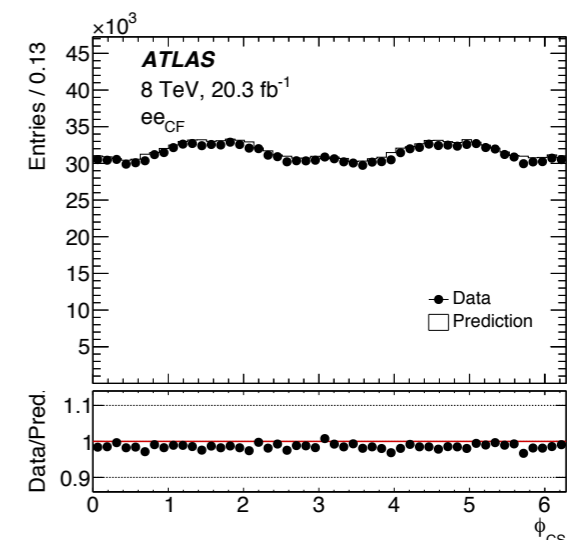
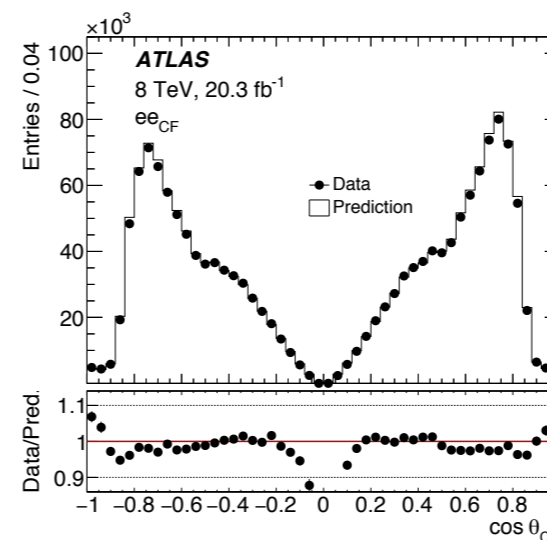
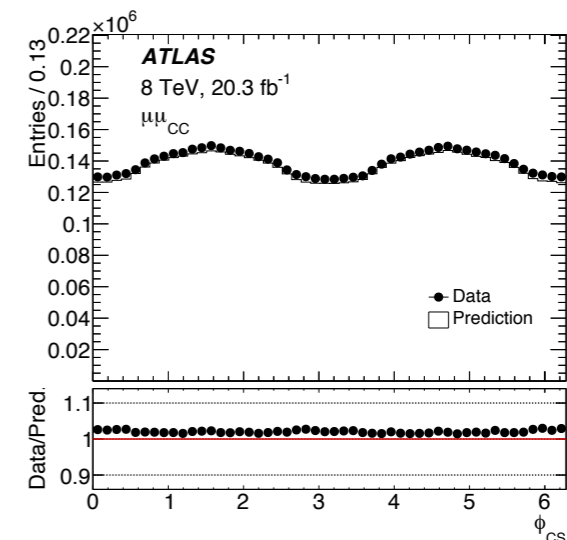
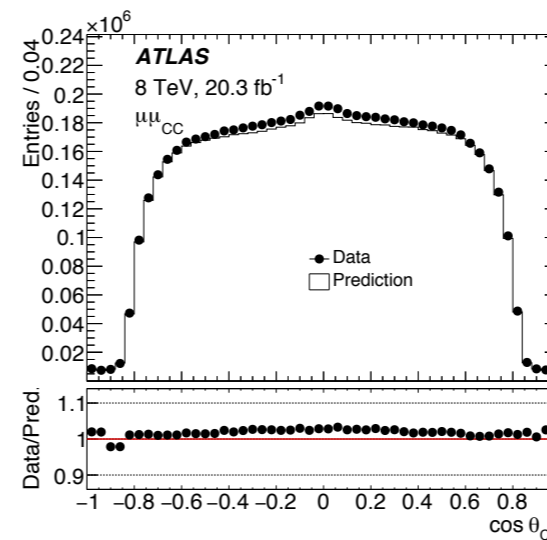
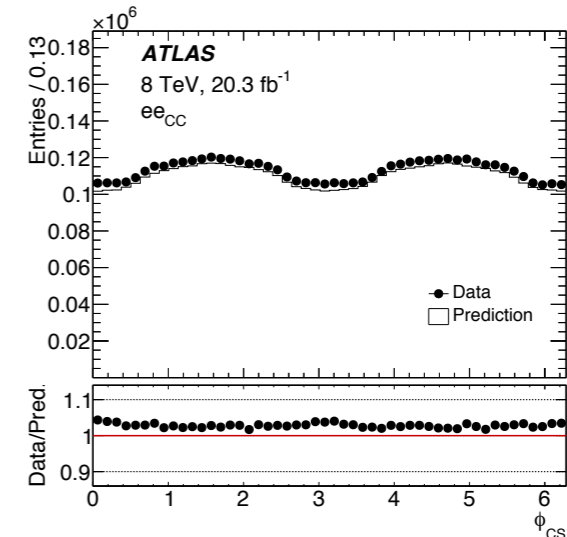
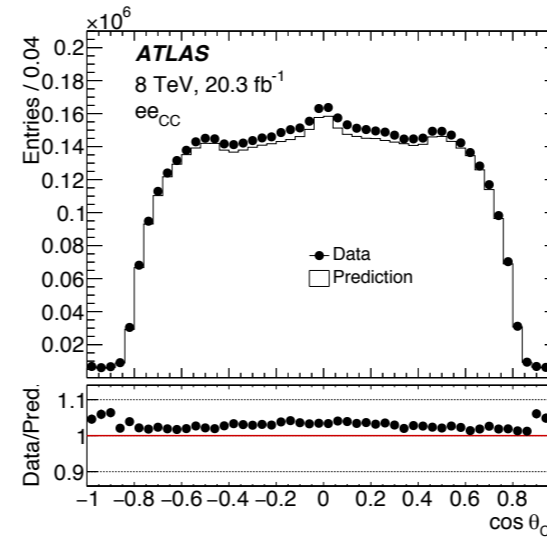


Background - CMS

- Background contribution ranges from $\sim 0.1\%$ at low q_T to $\sim 1.5\%$ at high q_T .
- $t\bar{t}$, $\tau\tau$, WW , tW , and W +jets production are estimated from data using lepton flavor universality.
 - Most of these backgrounds typically have two prompt leptons, which may have the same flavor.
 - W +jets is flavor asymmetric, **small contribution**
 - Assume that the ratio of the number of oppositely charged background $\mu\mu$ and $e\mu$ events is the same in data and simulation.
 - Use the ratio of the $e\mu$ yields in data and simulation after applying muon and electron selection criteria to normalize the simulation to data.

Angular distributions modeling in MC - ATLAS

- The data and MC distributions are not normalized to each other, resulting in normalization differences at the level of a few percent.
 - The measurement of the angular coefficients is, however, independent of the normalization between data and simulation in each bin of p_T^Z .
- The differences in shape in the angular distributions reflect the mis-modelling of the angular coefficients in the simulation



More on template methodology - CMS

- A_i are measured in 8 bins of q_T and 2 bins of $|\eta|$, by fitting the two-dimensional $(\cos \theta_*, \varphi_*)$ distribution in data with a linear combination of templates.
- The templates are built for each coefficient A_i by reweighting the simulation at generator level to the corresponding angular distribution.
 - The templates are based on reconstructed muons,
 - Incorporate the effects of resolution, efficiency and acceptance.
- Template built for the term $(1 + \cos^2 \theta_*)$ also.
- An additional template, with shape and normalization fixed, for backgrounds.
- A binned maximum-likelihood method with Poisson uncertainties is employed for the fit.
- $A_5, A_6,$ and A_7 are set to zero and excluded from the fit.
- Since A_0 through A_4 are sign invariant in φ_* , the absolute value $|\varphi_*|$ is used.
- The fit is made in 12×12 equidistant bins in $\cos \theta_*$ and $|\varphi_*|$.
- The statistical uncertainties from the fit are confirmed by comparison with pseudo-experiments.

Uncertainties - ATLAS

Stat.

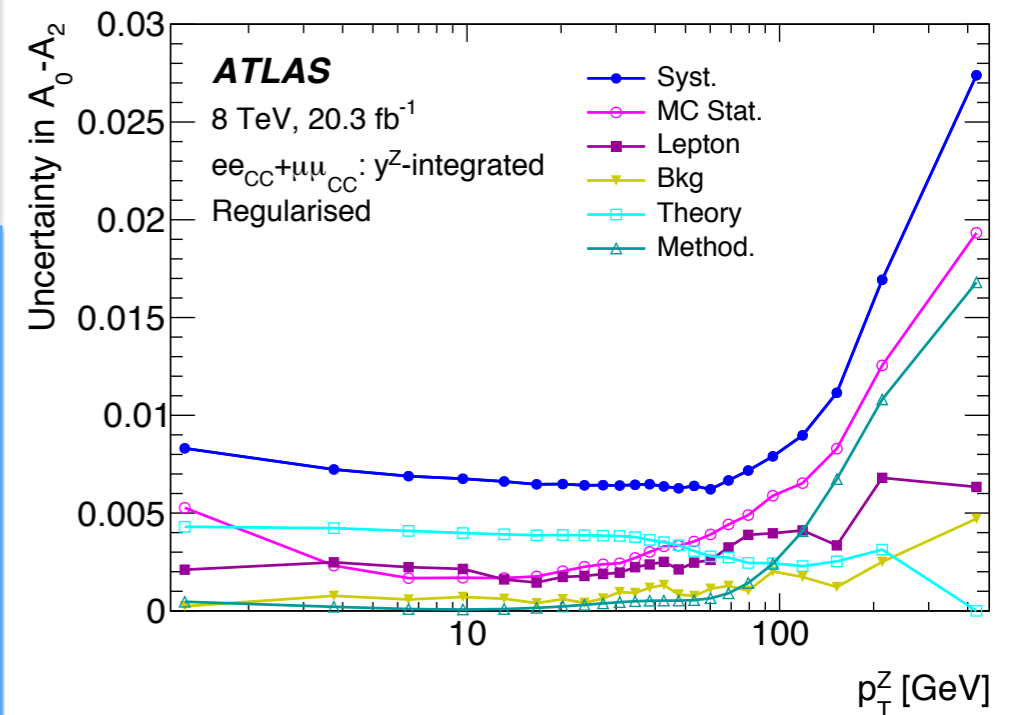
- Uncertainties from data and MC sample size
 - The amount of available data is the largest source of uncertainty

Experimental Syst.

- Lepton-related
 - Reconstruction, identification, trigger, electron mis-charge rate, efficiencies are applied MC
- Background-related:
 - Multijet normalization in each p_{Tl} bin and systematic using alternative criteria to define the multijet templates.
 - top+electroweak: 20% systematic
- Other experimental:
 - event pileup, detector misalignments, integrated luminosity $\pm 2.8\%$

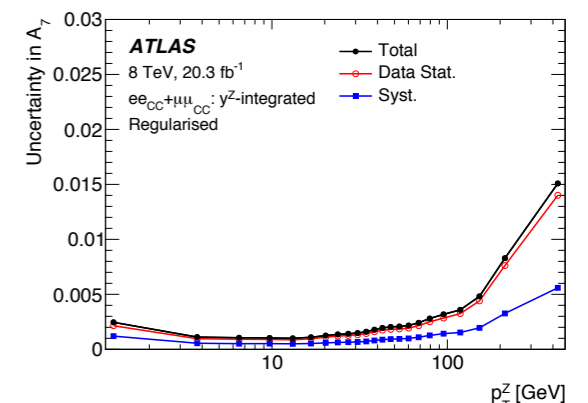
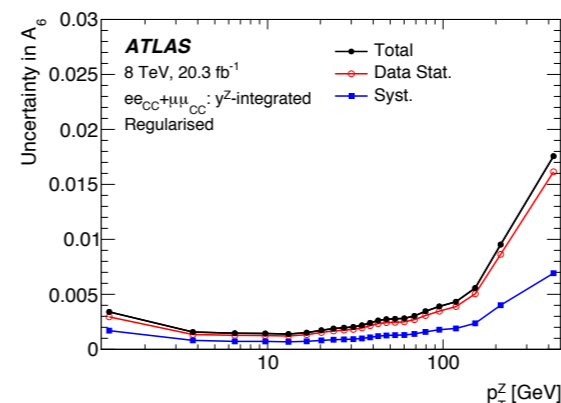
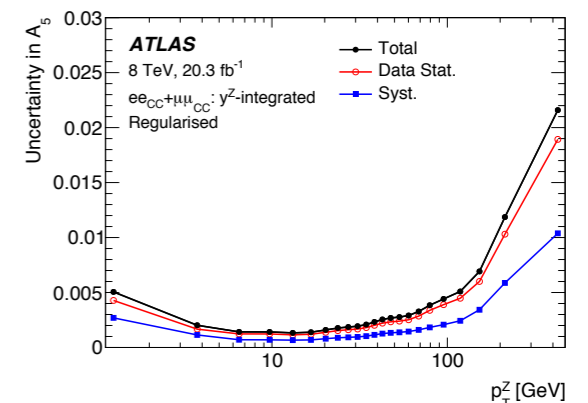
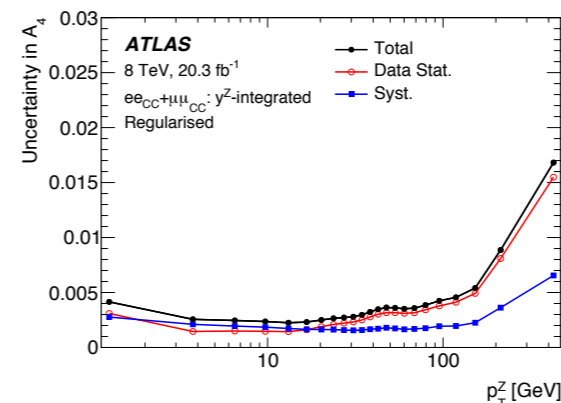
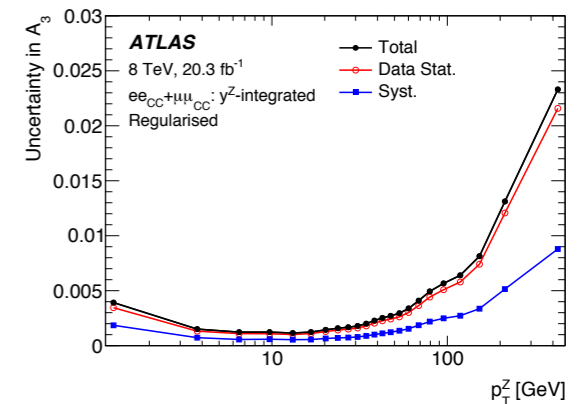
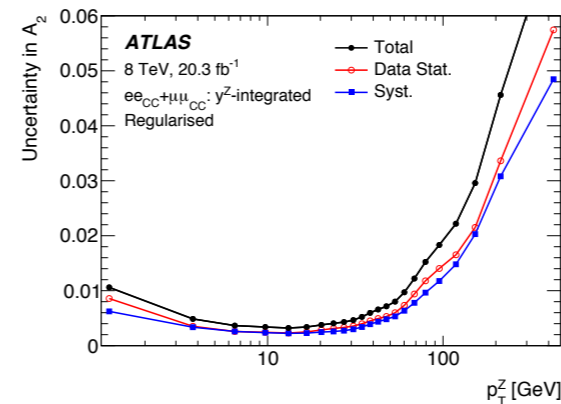
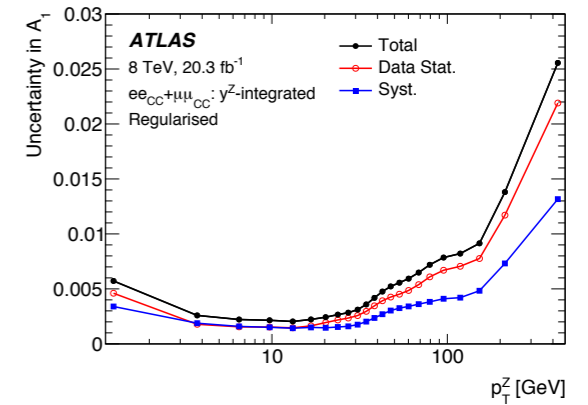
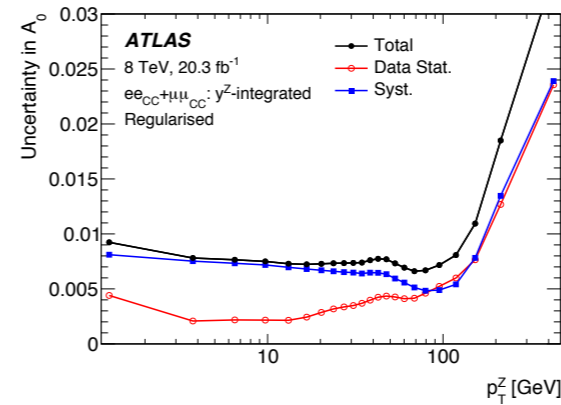
Theory Syst.

- QCD scale negligible:
 - Varying factorisation and renormalisation scale in the region $|y_Z| > 3.5$
- PDF (**the only non-negligible source of theoretical systematic uncertainty - especially for A_0 at low p_{TZ}**):
 - Computed with the 52 CT10 eigenvectors representing 26 independent sources.
 - Events are also reweighted using NNPDF2.3 and MSTW and are treated as independent systematics
- Parton showers:
 - The Powheg + Herwig samples are used to compute an alternative set of templates
- Event generator:
 - New set of templates from reweighting Yll of the nominal PowhegPythia8 to Sherpa
- QED/EW corrections negligible



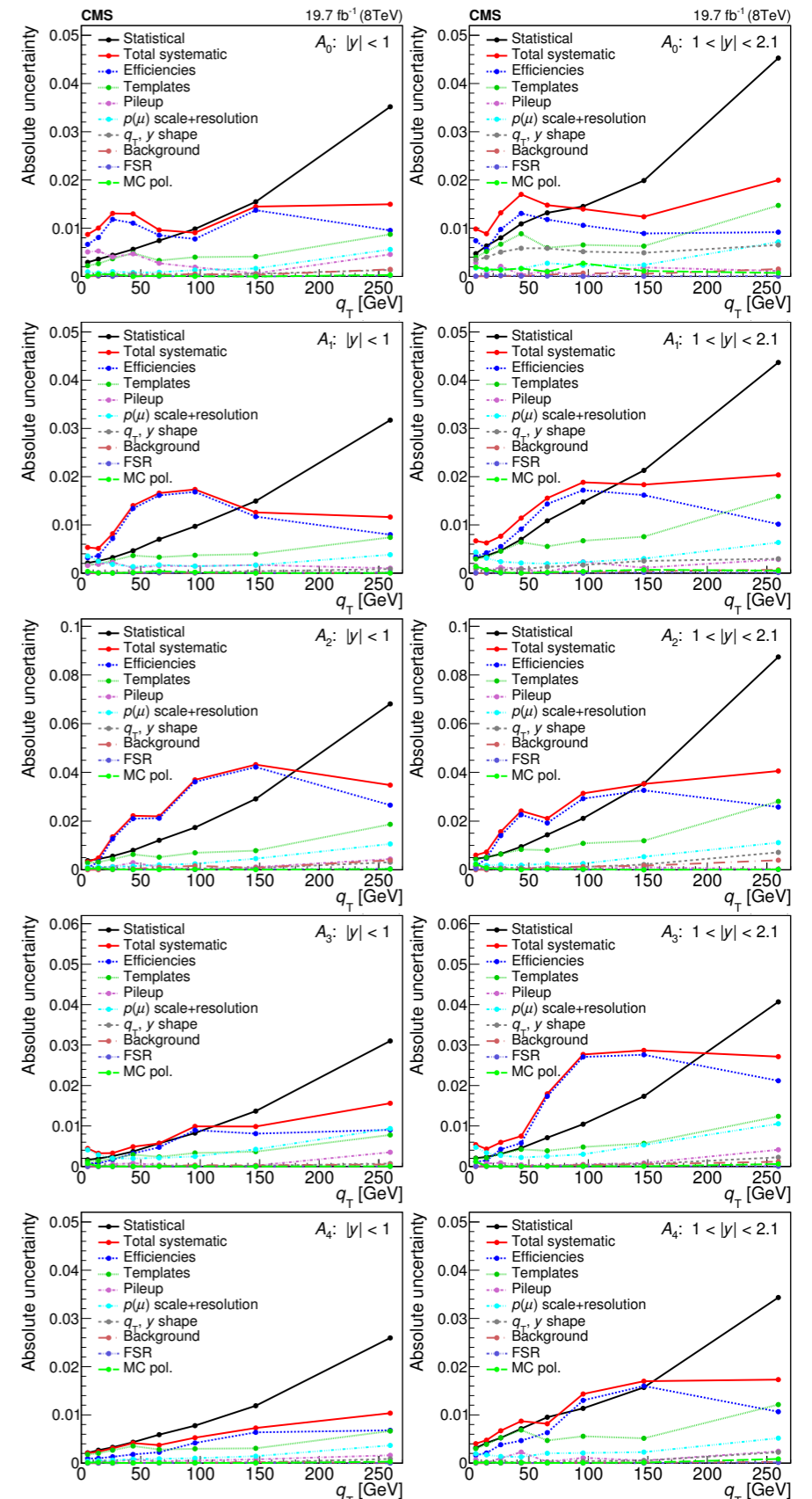
Uncertainties - ATLAS

- Statistics dominant uncertainty of the A_i coefficients is in most cases
 - Exception is A_0 coefficient where PDF and electron efficiency dominate for p_{TZ} values below 80 GeV.
- The next largest uncertainty is due to the signal MC statistical uncertainty
- Regularization can be significant for A_0 and A_2
 - Event migration between p_{TZ} bins leads to anti-correlations between A_i in neighbouring bins enhance statistical fluctuations
 - A_i spectra are regularised by multiplying the unregularised likelihood by a Gaussian penalty term, (function of the significance of higher-order derivatives of the A_i with respect to p_{TZ})



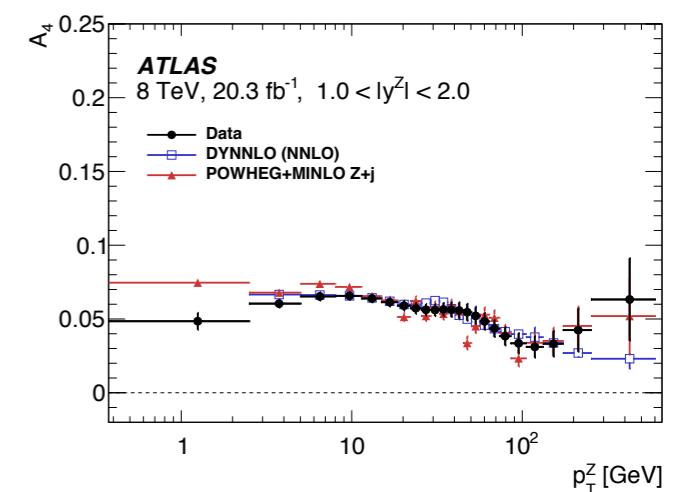
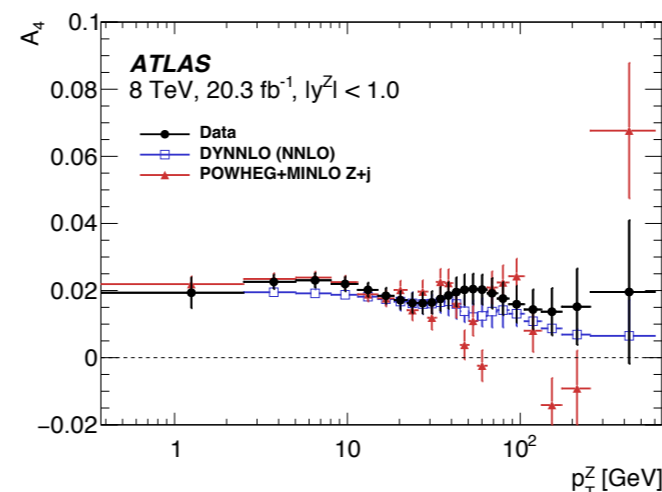
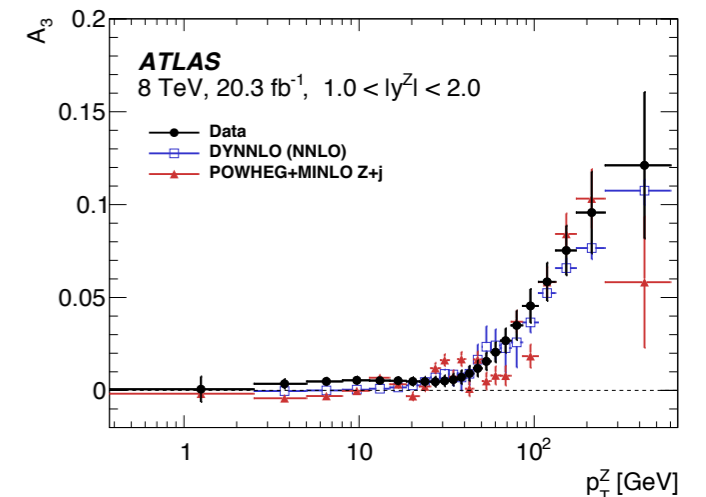
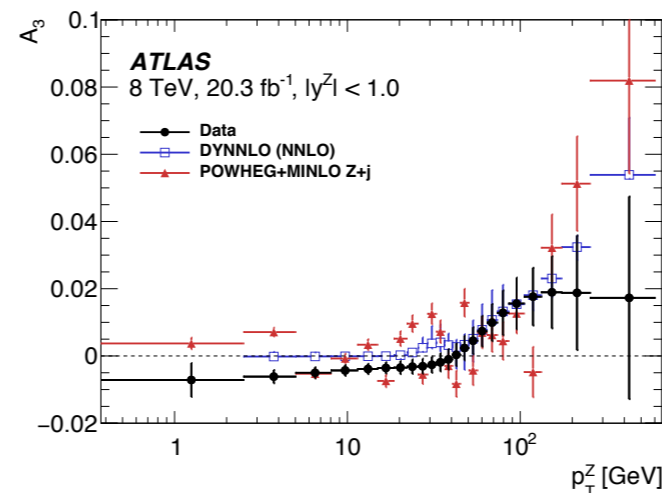
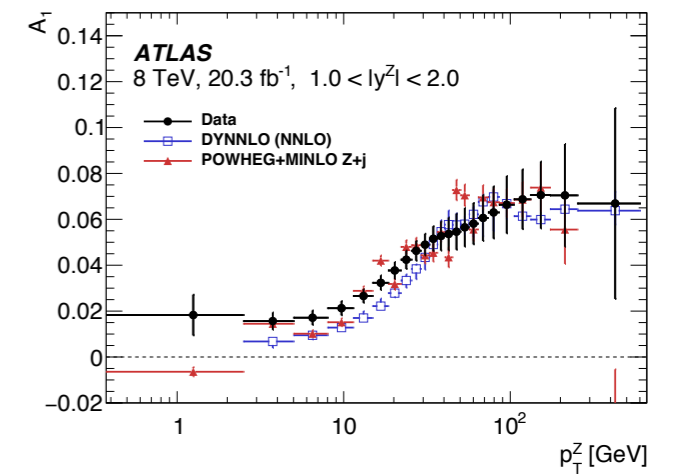
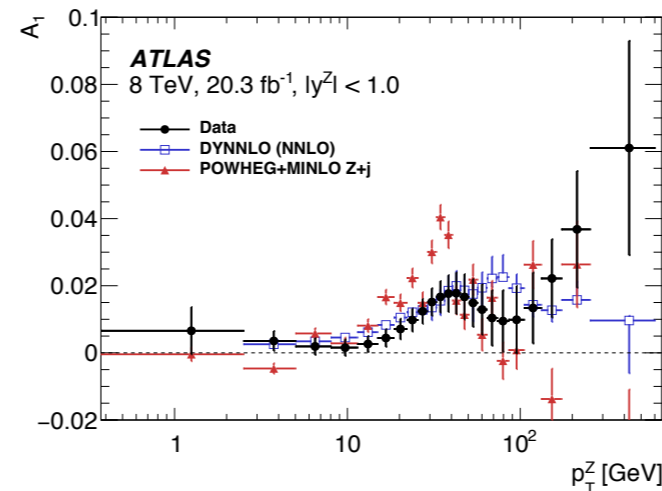
Uncertainties - CMS

- Dominant is the muon efficiency
 - includes the trigger, track reconstruction, isolation, and identification.
- Uncertainty from statistical precision of the templates, estimated using pseudo-experiments.
- Pileup uncertainty is estimated by varying the cross section of the minimum bias events by $\pm 5\%$.
- A systematic uncertainty is assessed to take into account possible global offsets from the peak position of the Z boson mass.
- Systematics for the background estimated by varying the normalization scale factor of the $e\mu$ sample by 10% and the yields of WZ and ZZ events by 50%.
- Acceptance uncertainty, related to the values of A_i assumed in the simulation, is estimated by reweighting with the fitted values of A_i , and the difference in results is included as a systematic uncertainty.
- **Generally, the statistical uncertainties dominate in the highest bins in q_T , whilst the systematic uncertainty in the efficiency tends to be the most important elsewhere.**



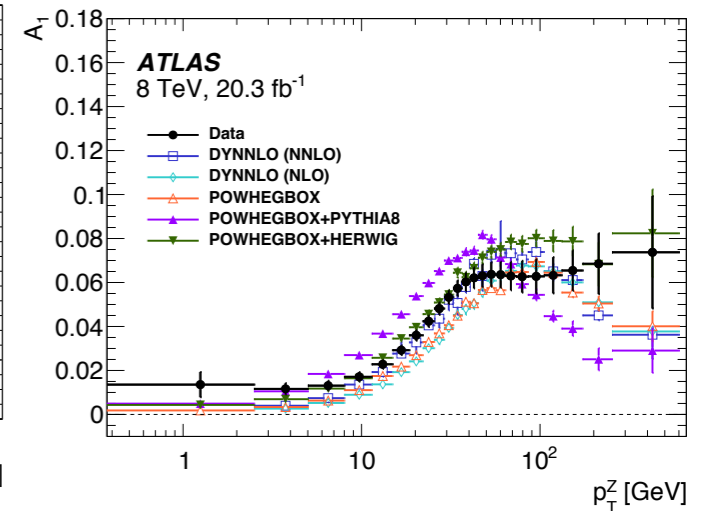
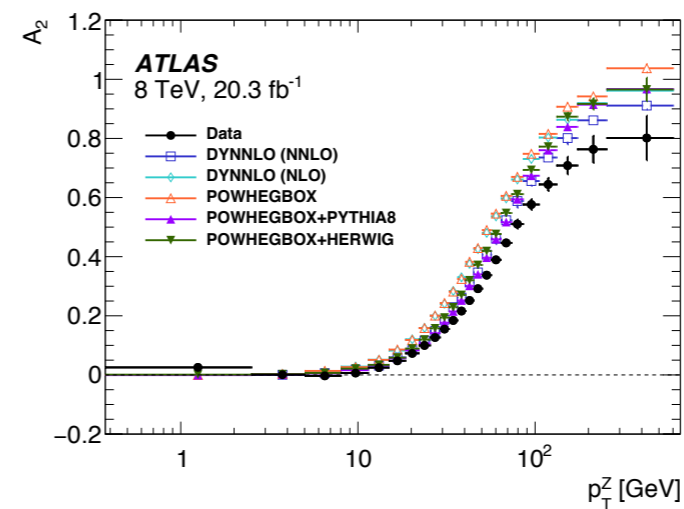
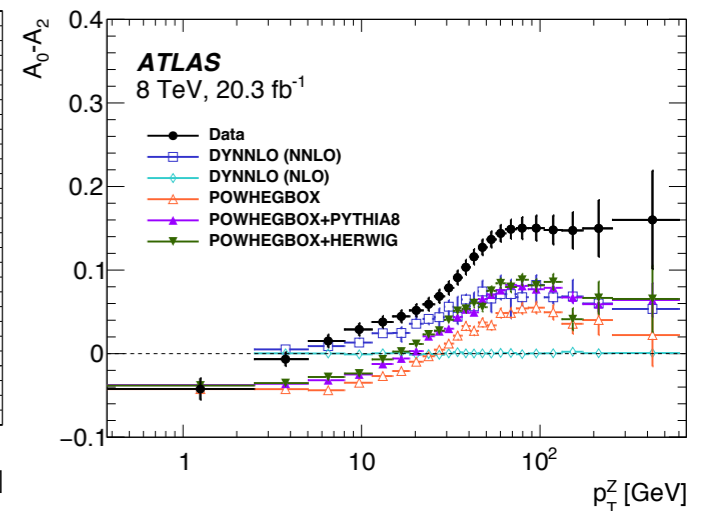
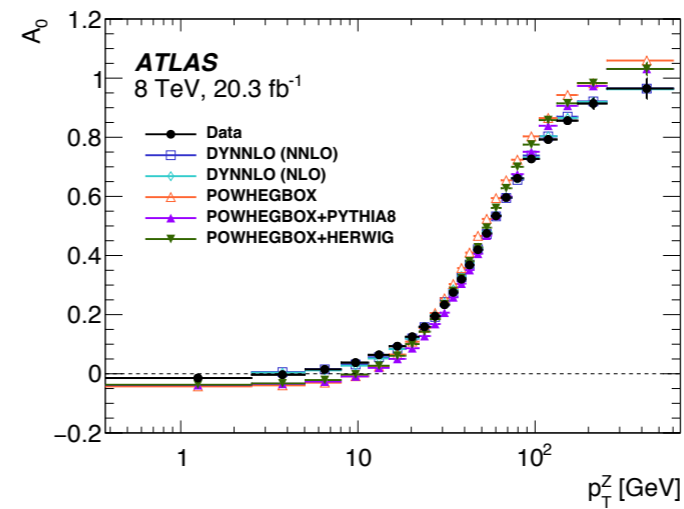
Results in y -bins - ATLAS

- A_1 , A_3 , and A_4 overall, the predictions and the data agree for all three y_Z bins.
 - The only coefficients that display any significant y_Z dependence
- For high values of $p_{T,Z}$, the A_1 and A_3 increase with y_Z .
- Strong dependence of the value of the A_4 on $|y_Z|$ is mostly a consequence of the approximation made for the interacting quark direction in the CS reference frame
 - The impact of this decreases at higher values of $|y_Z|$, and the measured and expected values of the A_4 increase



Effect of parton-shower modelling - ATLAS

- Comparison with DYNNLO at NLO and NNLO, PowhegBox (without parton shower), PowhegPythia8 and Herwig
- **DYNNLO at NLO and Powheg without parton shower agree for A1 and A2.**
- For A2 adding parton-shower simulation to the Powheg brings the predictions closer to DYNNLO at NNLO.
 - This is consistent with the assumption that the parton-shower model emulates higher-order effects, although the discrepancy between the measurements and the parton-shower models is larger than that with DYNNLO at NNLO.
- DYNNLO at NLO and NNLO agree well with the data measurements for the A0 but overestimate the rise of the A2 at higher values of $p_{T,Z}$
- A1 displays significant differences between the Pythia8 and Herwig



ϕ^* measurement

Signal MC samples - ATLAS

- ResBos (Evgen only):
 - Does not include hadronic activity in the event nor of FSR.
 - Initial-state QCD corrections to Z-boson production simulated at approximately NNLO accuracy using approximate NNLO Wilson coefficient functions.
 - γ^* from Z/ γ^* interference are simulated at NLO
 - Uses a resummed treatment of soft-gluon emissions at NNLL accuracy.
 - It uses the GNW parameterisation of non-perturbative effects at small p_T^Z
 - uses CT14 NNLO PDF
- Dynnlo (Evgen only):
 - simulates initial-state QCD corrections to NNLO.
 - CT10 NNLO PDF
 - Uses G_μ electroweak parameter scheme.
 - Does not account for the effects of multiple soft-gluon emission and therefore is not able to make accurate predictions at low \sqrt{s} and p_T^Z
- Powheg+Pythia(Evgen only):
 - Uses the AZNLO tune which includes the ATLAS 7 TeV \sqrt{s} and p_T^Z results in a mass region around the Z peak.
 - The sample uses Pythia8 and CTEQ6L1 PDF for the parton shower, while CT10 is used for the Powheg calculation.
- Powheg+Pythia (Full Simulation):
 - CT10 PDFs interfaced to Pythia with the AU2 Tune and Photos for FSR.
- Powheg+Herwig (Full Simulation):
 - Herwig for parton shower and hadronisation, Jimmy for the underlying event, and Photos for FSR
- Sherpa (Full Simulation):
 - Has its own implementation of the parton shower, hadronisation, underlying event and FSR, with CT10 PDF.

Signal MC- CMS 8,13TeV

Signal MC at 8 TeV analysis:

- Baseline: MADGRAPH at LO matrix element generator
 - includes up to 4 extra partons in the calculation
 - Used to estimate the efficiency and to unfold the data
 - PDF set CTEQ6L1
 - Parton shower and hadronisation are implemented by PYTHIA6 with the kT-MLM matching scheme the Z2* tune for the underlying event
- POWHEG (NLO) with the CT10NLO PDF interfaced with PYTHIA6 and the Z2* tune
- POWHEG (NLO) with the CT10NLO PDF interfaced with PYTHIA8 and the CUETP8M1 tune using NNPDF2.3 LO PDF
- RESBOS (resummed NNLL/NLO QCD) with CT10NLO PDF
- MADGRAPH5 aMC@NLO (NLO) with the NNPDF3.0 NLO PDF and PYTHIA8 for the parton shower and FxFx merging scheme

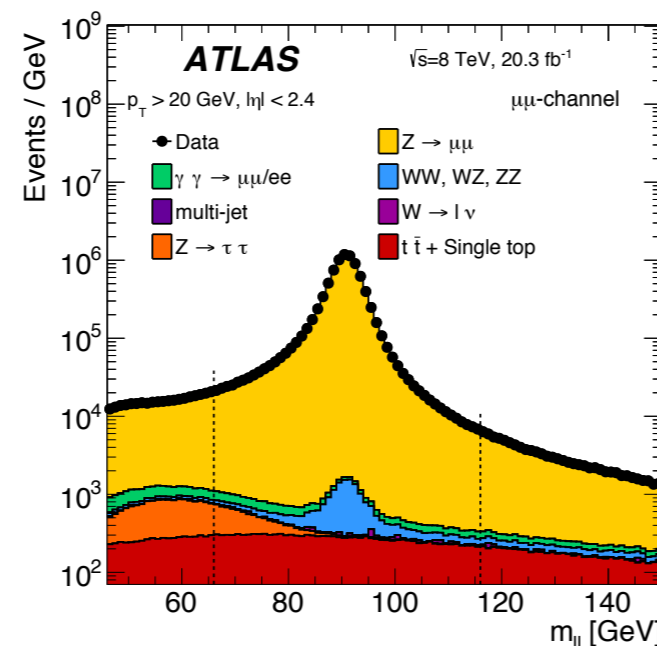
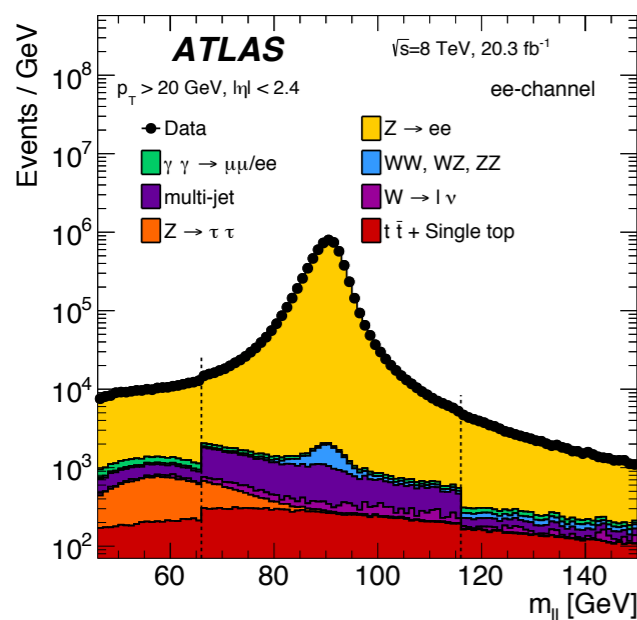
Signal MC at 13 TeV analysis:

- Baseline: MADGRAPH5 AMC@NLO with NLO matrix elements for final states with up to 2 additional partons
 - NNPDF 3.0 PDFs are used
- POWHEG +Pythia8 (NLO) for the parton shower and hadronization with the TuneCUETP8M1
- FEWZ (NNLO QCD) and NNPDF 3.0 PDFs. The renormalization and factorization scales are set to the mass of the Z boson. Electroweak NLO corrections included.

Event Selections - ATLAS

| Particle-level definitions (Treatment of final-state photon radiation) | |
|--|--|
| electron pairs | dressed; Born |
| muon pairs | bare; dressed; Born |
| combined | Born |
| Fiducial region | |
| Leptons | $p_T > 20 \text{ GeV}$ and $ \eta < 2.4$ |
| Lepton pairs | $ y_{\ell\ell} < 2.4$ |
| Mass and rapidity regions | |
| $46 \text{ GeV} < m_{\ell\ell} < 66 \text{ GeV}$ | $ y_{\ell\ell} < 0.8$; $0.8 < y_{\ell\ell} < 1.6$; $1.6 < y_{\ell\ell} < 2.4$ (ϕ_{η}^* measurements only) |
| | $ y_{\ell\ell} < 2.4$ |
| $66 \text{ GeV} < m_{\ell\ell} < 116 \text{ GeV}$ | $ y_{\ell\ell} < 0.4$; $0.4 < y_{\ell\ell} < 0.8$; $0.8 < y_{\ell\ell} < 1.2$; $1.2 < y_{\ell\ell} < 1.6$; $1.6 < y_{\ell\ell} < 2.0$; $2.0 < y_{\ell\ell} < 2.4$; $ y_{\ell\ell} < 2.4$ |
| $116 \text{ GeV} < m_{\ell\ell} < 150 \text{ GeV}$ | $ y_{\ell\ell} < 0.8$; $0.8 < y_{\ell\ell} < 1.6$; $1.6 < y_{\ell\ell} < 2.4$ (ϕ_{η}^* measurements only) |
| | $ y_{\ell\ell} < 2.4$ |
| Very-low mass regions | |
| $12 \text{ GeV} < m_{\ell\ell} < 20 \text{ GeV}$ | } $ y_{\ell\ell} < 2.4, p_T^{\ell\ell} > 45 \text{ GeV}, p_T^{\ell\ell}$ measurements only |
| $20 \text{ GeV} < m_{\ell\ell} < 30 \text{ GeV}$ | |
| $30 \text{ GeV} < m_{\ell\ell} < 46 \text{ GeV}$ | |

- Electron Selection:
 - $p_T > 20 \text{ GeV}$ and $|\eta| < 2.4$, but excluding $1.37 < |\eta| < 1.52$.
 - 'medium' selection criteria
 - Exactly two electron candidates
 - Isolated, $I_e < 0.2$ (cone $\Delta R < 0.4$)
- Muon selection:
 - $p_T > 20 \text{ GeV}$ and $|\eta| < 2.4$.
 - Track-quality requirements
 - Isolated, $I_{\mu} < 0.1$ (cone $\Delta R < 0.2$)
 - Exactly two muon candidates of opposite charge
- Multijet background from data
- All other backgrounds from MC



Event Selections - CMS 8,13TeV

- Lepton Selection 8TeV:

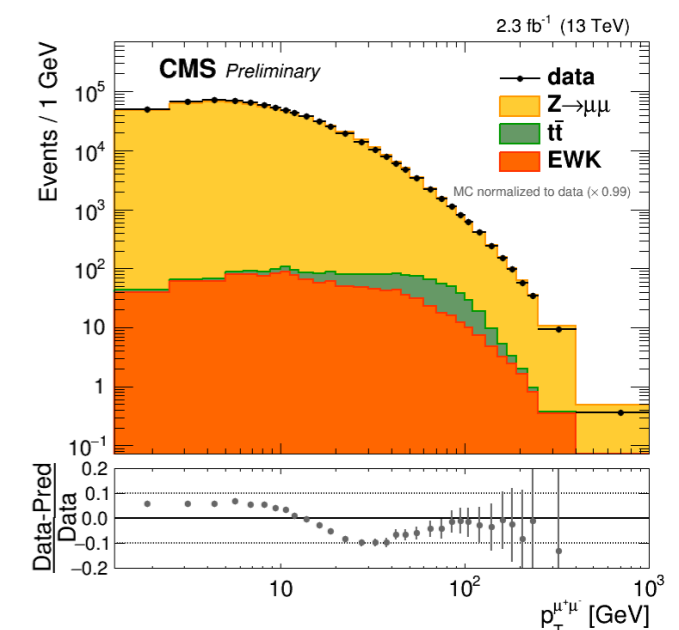
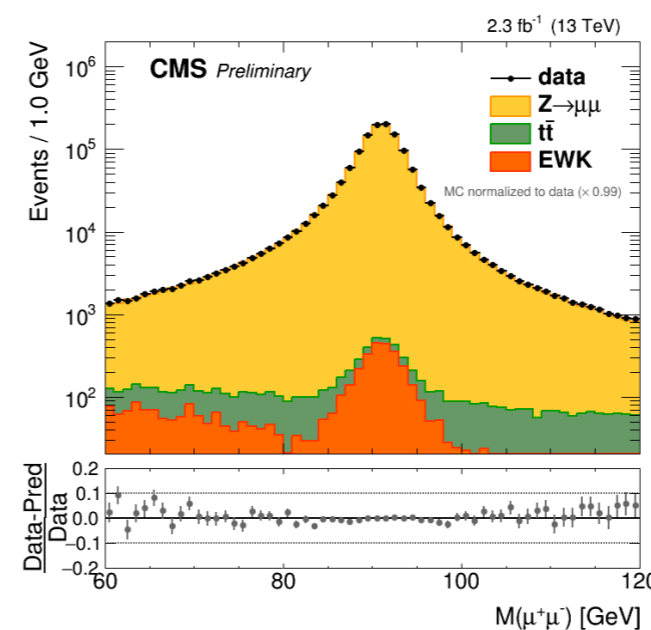
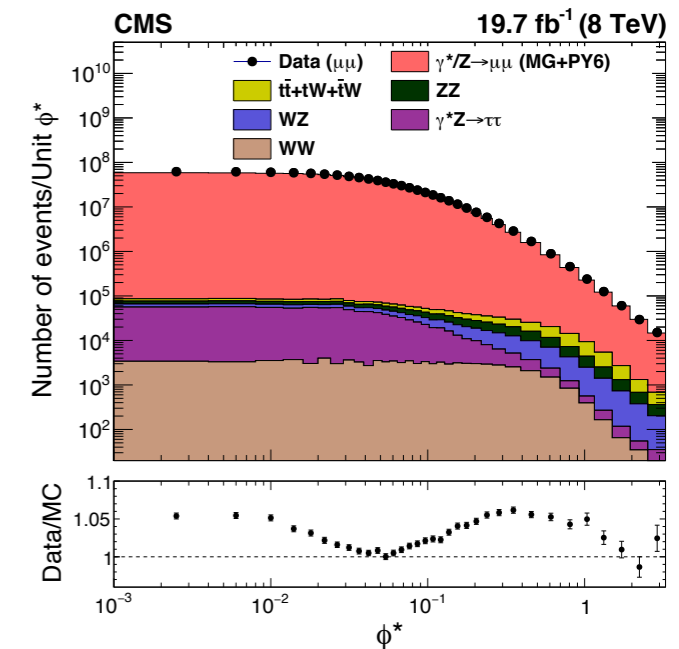
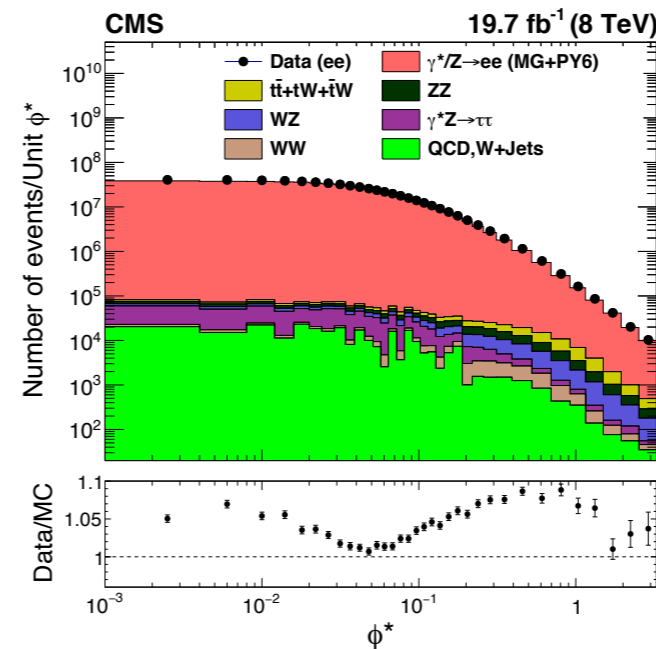
- $p_{T1} > 30$ GeV and $|\eta_1| < 2.1$, $p_{T2} > 20$ GeV and $|\eta_2| < 2.4$. but excluding $1.444 < |\eta| < 1.566$ for electrons
- $d_0 < 0.02$ cm, $z_0 < 0.1$ (0.5)cm electron (muon)
- $60 < m_Z < 120$ GeV
- Isolation electrons (muons) in $dR < 0.3$ (0.4) with $I < 0.15$ (0.12)
- opposite sign muons
- $\phi^* < 3.227$ to keep the stat. and syst. uncertainties comparable in the relevant bin

- Background only 0.6% and 0.5% for electron and muon**

- Wjets +MultiJet from Data, others from MC

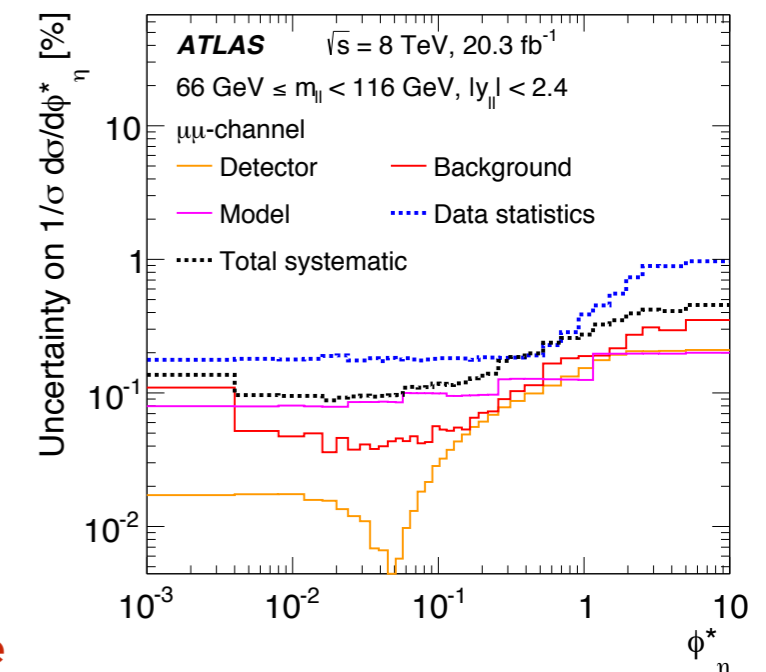
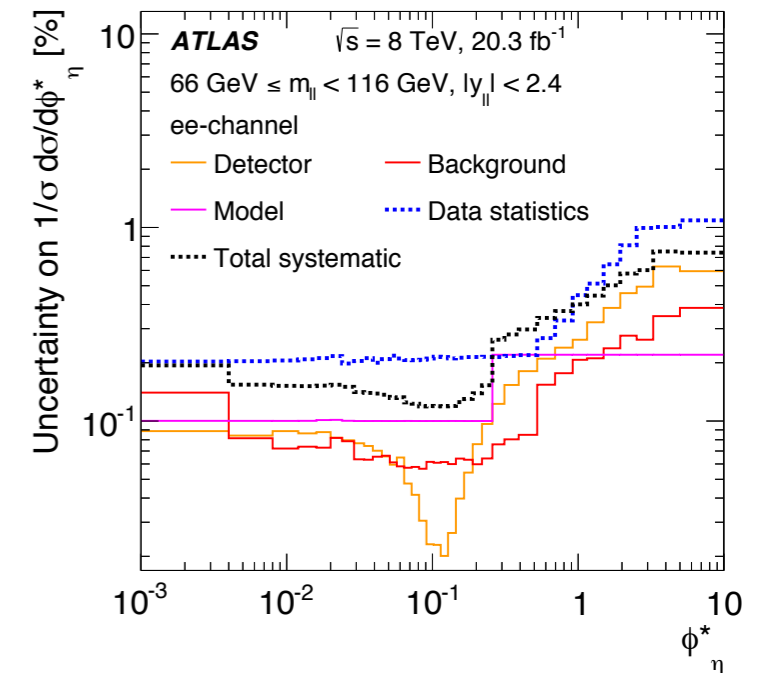
- Muon Selection 13 TeV:

- $p_T > 25$ GeV and $|\eta| < 2.4$
- Isolation: $dR < 0.4$ with $I < 0.15$
- $60 < m_Z < 120$ GeV



Uncertainties - ATLAS

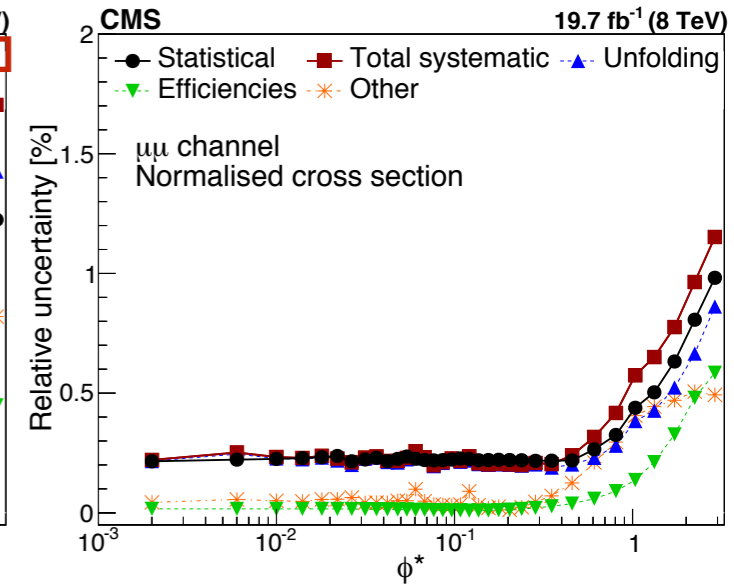
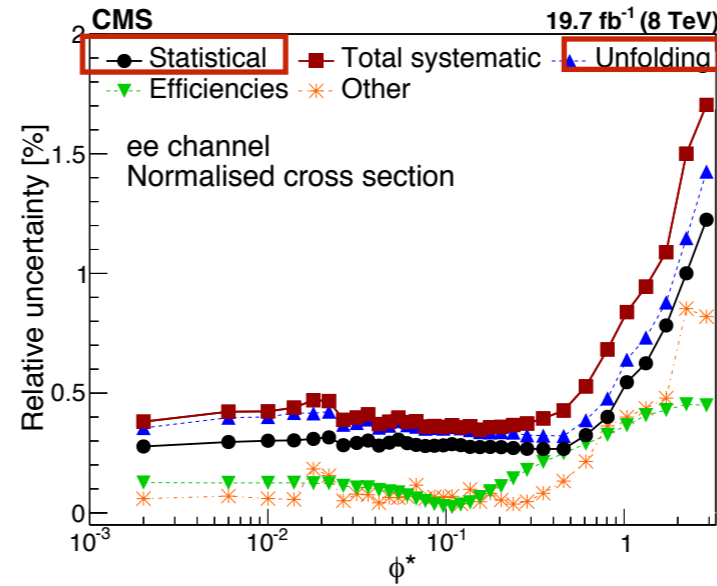
- **Statistical uncertainties on the data and MC samples used to correct the data (considered as uncorrelated between bins and between channels) dominant in most kinematic regions**
- Systematics due to detector modelling:
 - lepton energy (electron) and momentum (muon) scales and their resolution
 - lepton reconstruction, identification, trigger and isolation efficiencies, d0 (very small)
 - pile-up distribution (small, but non-negligible contribution)
 - lepton angular resolution of an order similar to that of the pile-up
- Systematics due to background:
 - Due to varying the normalisation of each MC background within its theoretical cross-section (treated as correlated between channels).
 - Small in the mll region around the Z- boson peak, more significant in regions away from the peak.
 - Multi-jet background normalization obtained from template fits (treated as fully correlated between bins). Small contribution to the total uncertainty, important for the mll regions below the Z peak.
- Systematic due to the choice of signal MC
 - Central values from Powheg+Pythia and the difference in the results obtained when unfolding the data with Sherpa.
 - below the Z-boson mass peak significant contribution due to the differences in FSR modeling between Photos and Sherpa.
 - PDFs (negligible).
- Systematic on the integrated luminosity is 2.8% (negligible)
- **For ϕ^* the total systematic uncertainties at the Z-boson mass peak are at the level of around 1 per mille at low ϕ^* , rising to around 0.5% for high ϕ^***



Uncertainties - CMS 8,13 TeV

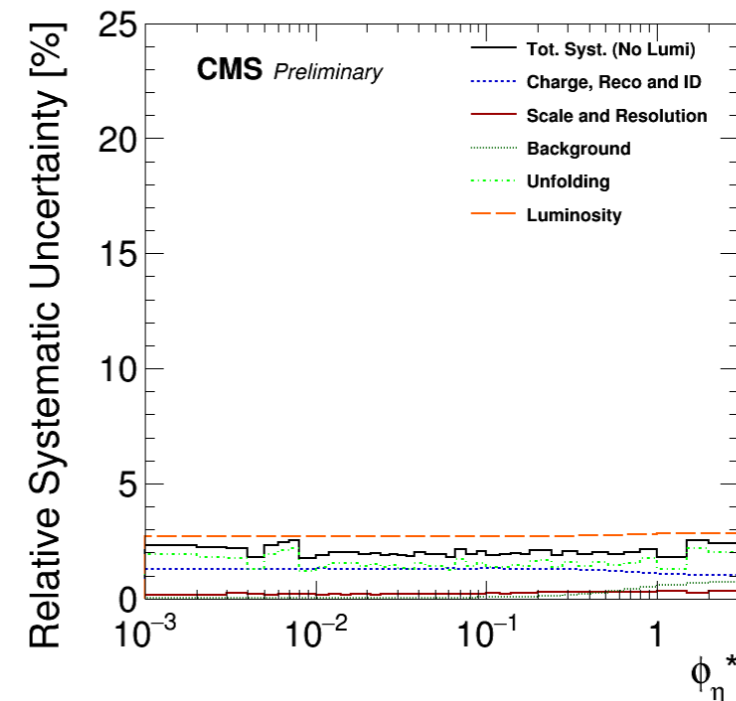
Uncertainties at 8 TeV analysis:

- **Integrated luminosity dominant 2.6%**
 - Uniform across all ϕ^* and $|\eta|$ bins (**relevant only for the absolute cross section measurements**)
- The unfolding uncertainty originates from the finite size of the MC signal sample used for the response matrix
 - $O(\text{stat uncertainty})$
- Lepton identification, isolation, and trigger efficiency values from the simulation.
- Electron energy scale affects all ϕ^* bins $\sim 0.15\%$ (0.06%) for the absolute (normalized) cross section measurement
- PDF uncertainties are negligible



Uncertainties at 13 TeV analysis:

| | |
|------------------------------------|------------|
| Lepton reco. & id. [%] | 1.3 |
| Bkg. subtraction / modeling [%] | 0.1 |
| Total experimental [%] | 1.3 |
| PDF [%] | 0.7 |
| QCD corrections [%] | 1.1 |
| EW corrections [%] | 0.4 |
| Theoretical Uncertainty [%] | 1.4 |
| Lumi [%] | 2.7 |
| Total [%] | 3.3 |



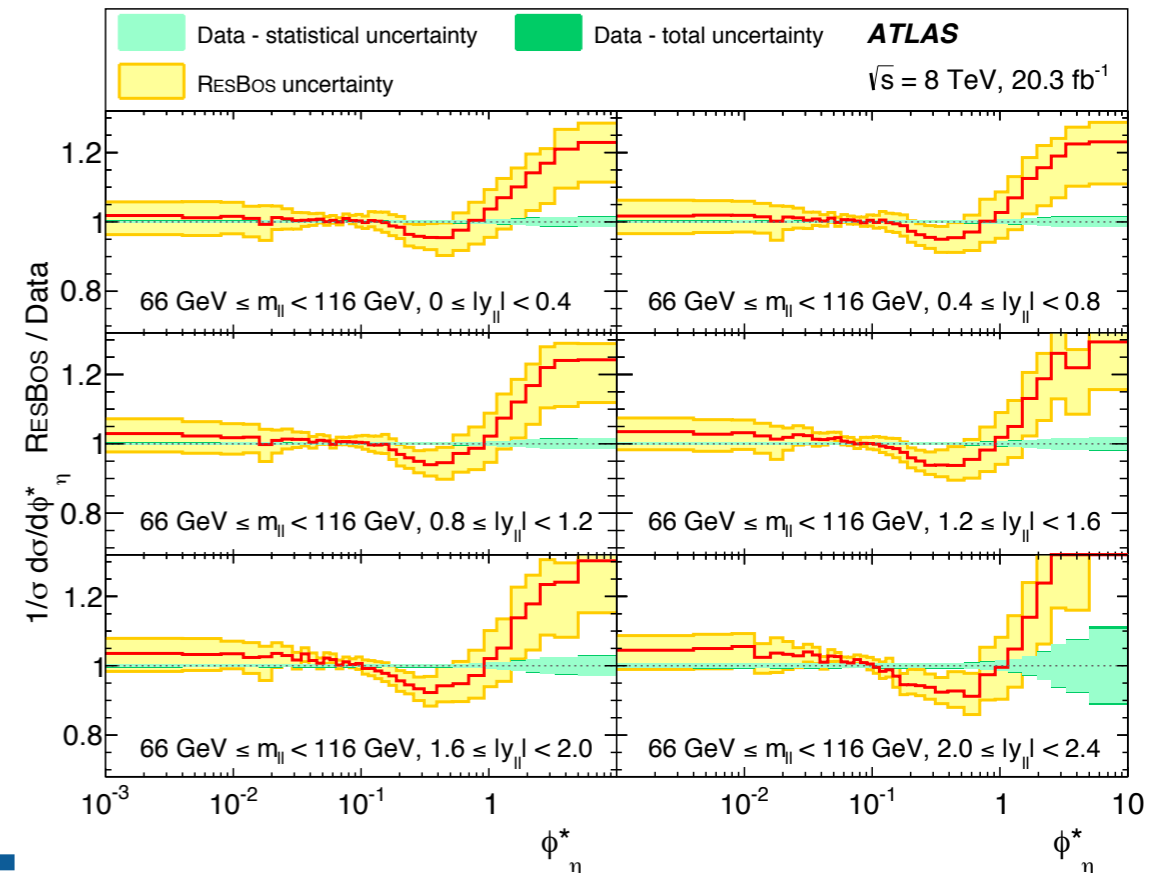
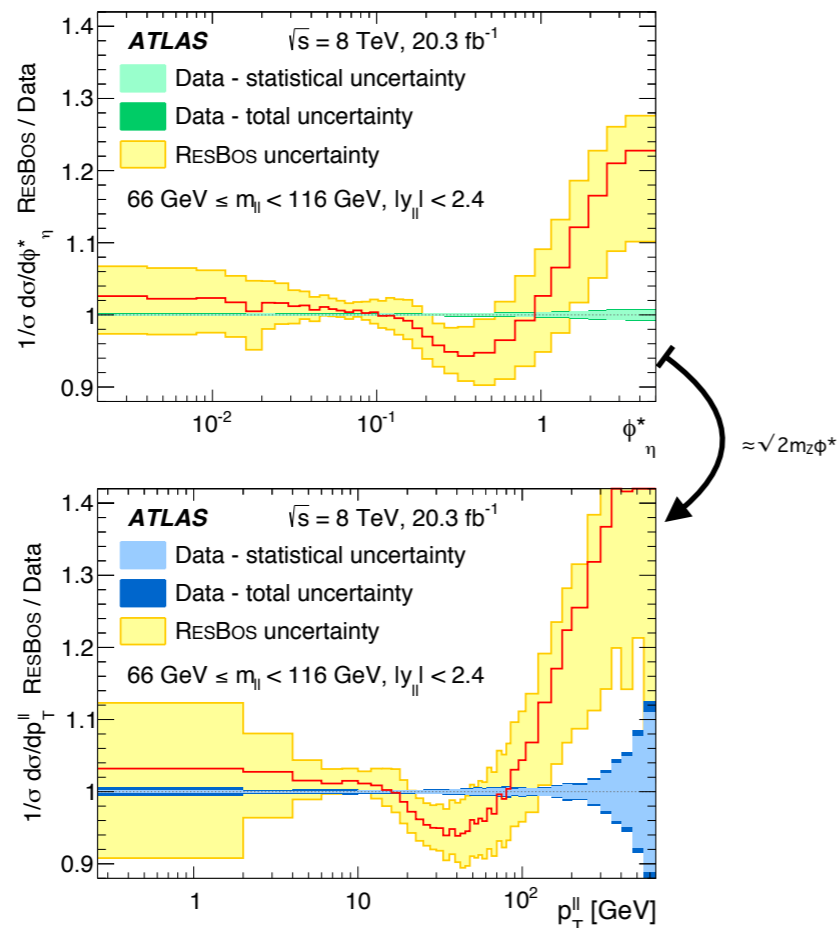
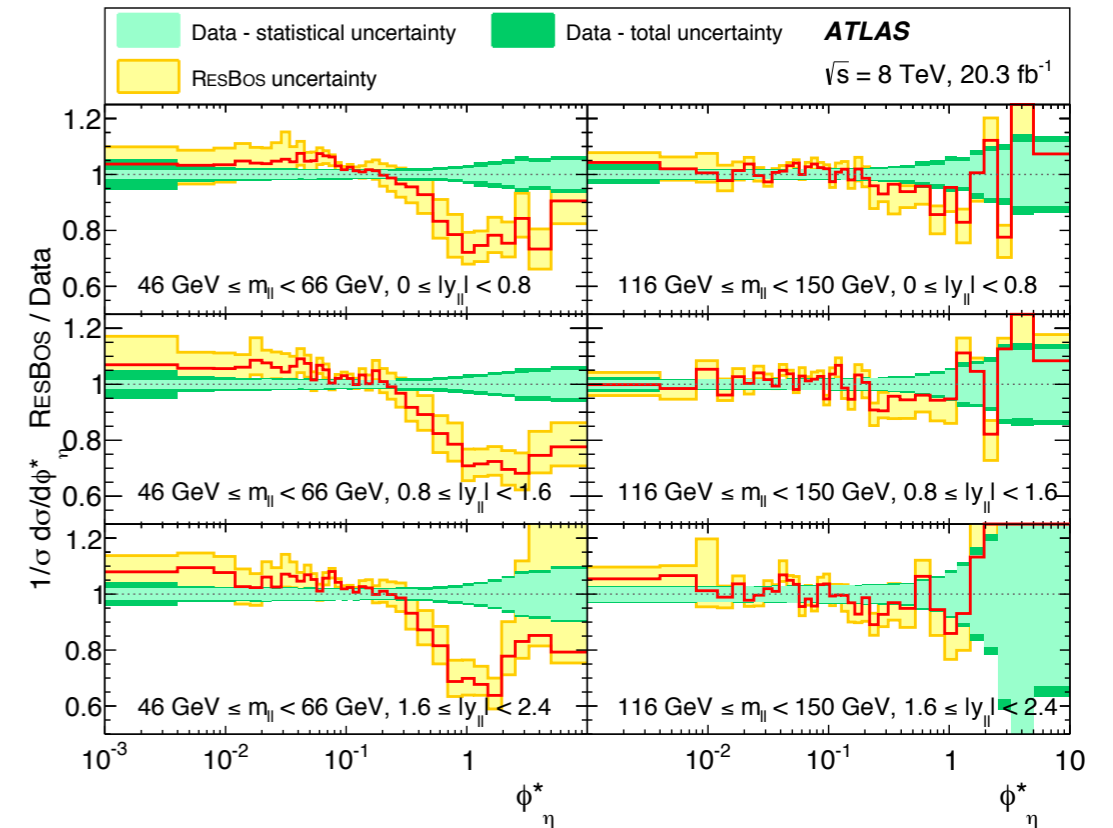
Uncertainties - LHCb 13 TeV

- Statistical precisions of the lepton efficiencies are assigned as systematic uncertainties.
- The uncertainties on the purity estimates treated as correlated between all bins
- The uncertainties on the FSR corrections are taken as uncorrelated between all bins.
- A systematic uncertainty on unfolding with different number of iterations is at the per-mille level in each bin

| Source | $\Delta\sigma_Z^{\mu\mu}$ [%] | $\Delta\sigma_Z^{ee}$ [%] |
|--------------------------------|-------------------------------|---------------------------|
| Statistical | 0.5 | 0.9 |
| Reconstruction efficiencies | 2.4 | 2.4 |
| Purity | 0.2 | 0.5 |
| FSR | 0.1 | 0.2 |
| Total systematic (excl. lumi.) | 2.4 | 2.5 |
| Luminosity | 3.9 | 3.9 |

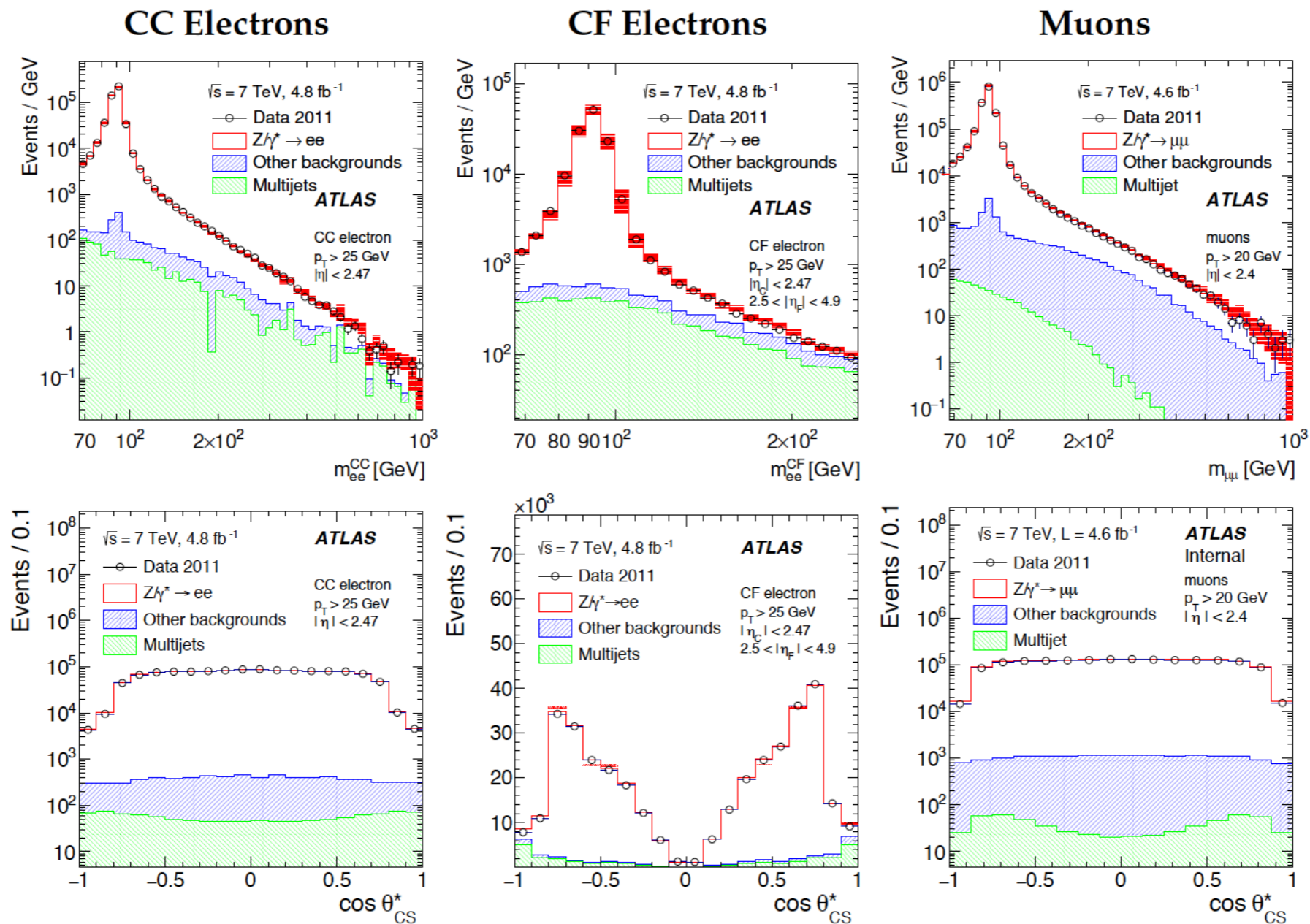
Results in y , p_T and mass bins

- For m_{ll} above the Z peak ResBos is consistent with the data within uncertainties for all values of φ^*
- For m_{ll} 46 to 66 GeV ResBos lies below the data for $\varphi^* > 0.4$.
 - known deficiency of ResBos is the lack of NNLO QCD corrections for the contributions from γ^* and from Z/ γ^* interference
- **Generally the evolution of the x-section wrt to y and mass is described well by Resbos**



A_{FB} measurement

Di-leptons Invariant mass and $\cos\theta^*$ - ATLAS 7 TeV



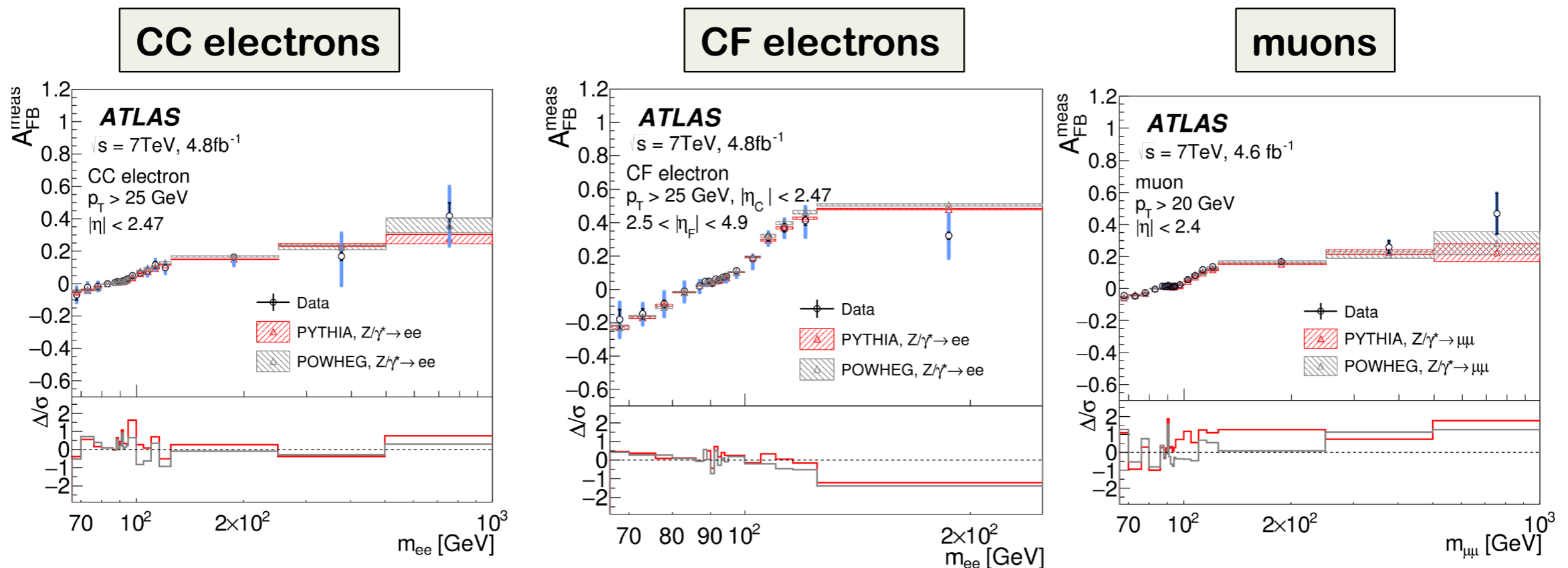
- Signal samples simulated with PYTHIA 6.4 (MSTW2008LO) and NLO POWHEG (MC) + PYTHIA6.4 for parton shower
- Background is taken from MC
 - For QCD multijet and like W+j use data-driven methods

Detector-level A_{FB} asymmetry - ATLAS 7 TeV

- Calculate A_{FB} from $\cos\theta^*$ distribution at detector level after background subtraction

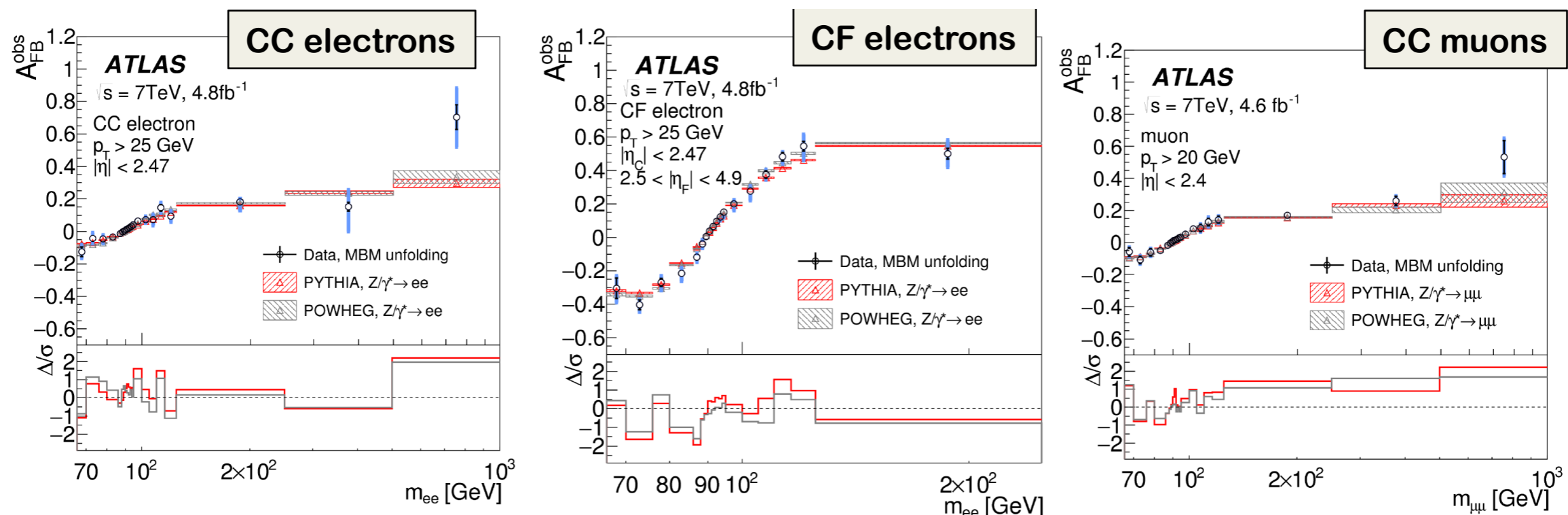
$$A_{FB} = \frac{N_{\cos\theta_{CS}^* \geq 0} - N_{\cos\theta_{CS}^* < 0}}{N_{\cos\theta_{CS}^* \geq 0} + N_{\cos\theta_{CS}^* < 0}}$$

- Good agreement with Pythia and Powheg predictions is found



Unfolding AFB from detector to particle level - ATLAS 7 TeV

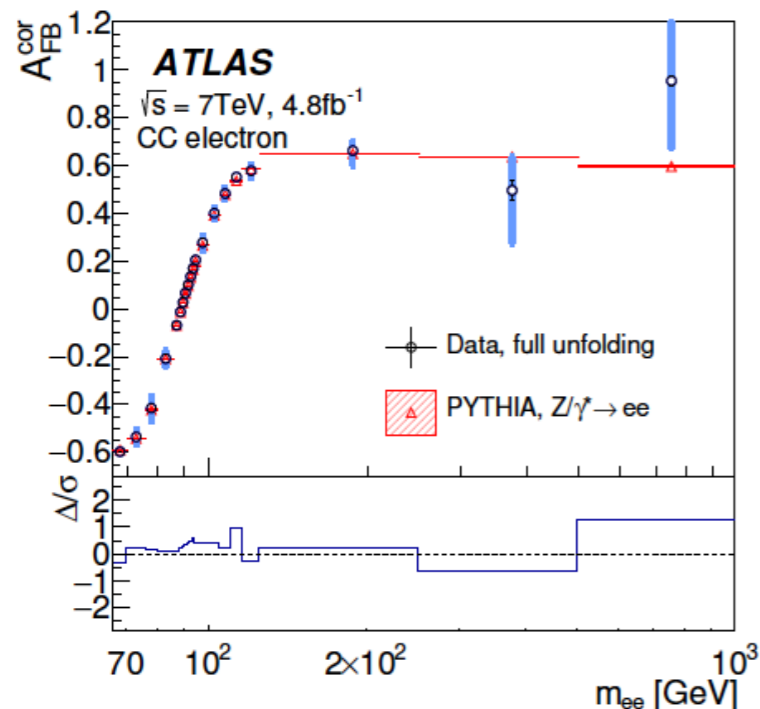
- Unfolding AFB at detector level to particle level using a Bayesian iterative method to compare with theoretical predictions
 - Response matrix built with Pythia6.4 MC signal samples to correct for 'mass bin migration effects':
 - Detector effects : finite resolution, lepton reconstruction efficiency • cross-check with PYTHIA LO MC
 - QED : radiative corrections or real photon in the final-state (FSR) • cross-check with SHERPA+PHOTON++ MC
 - NLO EWK corrections • cross-check with HORACE MC
 - NLO QCD effects cross-check with POWHEG simulated sample as pseudo-data and unfolding the asymmetry using the PYTHIA derived response matrix
 - All cross-check effects smaller than the statistical uncertainties



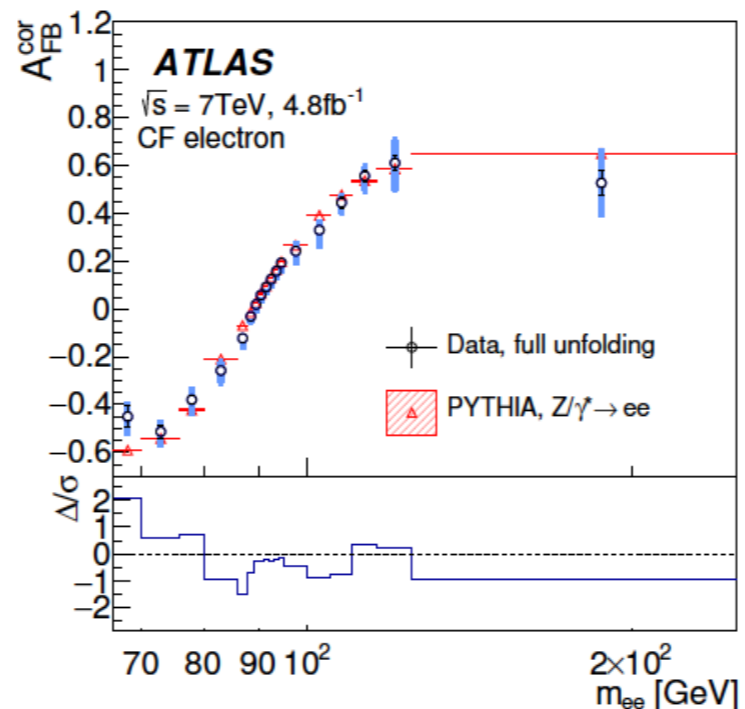
AFB corrected for dilution and acceptance - ATLAS 7 TeV

- Similar unfolding procedure using PYTHIA MC samples to remove also:
 - Dilution effect
 - Wrong choice for quark direction
 - Rely heavily on MC simulation, in particular on the precise PDFs knowledge
 - Geometrical acceptance correction to extrapolate to full phase-space
- Magnitude of the corrections bigger than previous steps
 - Dominated by the PDF systematic uncertainties

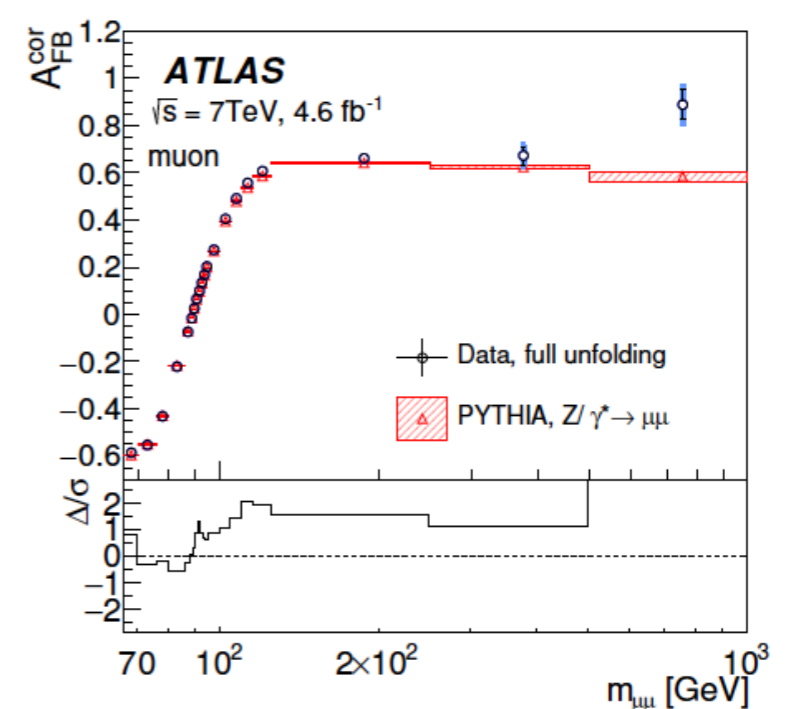
CC Electrons



CF Electrons



Muons



Systematics on AFB observed - ATLAS 7 TeV

- Sources of uncertainties:
 - Unfolding uncertainties from data reweighting and response matrix statistics
 - Energy scale and resolution
 - Background uncertainty from difference between methods (negligible in CC electrons and muons)
 - PDF uncertainties from CT10 error set.
 - For each error set the MC sample is reweighted, the response matrix calculated and unfolding is repeated
 - The results quoted at 68%CL
- No single dominating uncertainty overall**

| CC electrons | | | |
|-------------------------|-------------------------|--------------------------|--------------------------|
| Uncertainty | 66–70 GeV | 70–250 GeV | 250–1000 GeV |
| Unfolding | $\sim 1 \times 10^{-2}$ | $(2-5) \times 10^{-3}$ | $\sim 4 \times 10^{-4}$ |
| Energy scale/resolution | $\sim 7 \times 10^{-3}$ | $(0.5-2) \times 10^{-3}$ | $\sim 2 \times 10^{-2}$ |
| MC statistics | $\sim 5 \times 10^{-3}$ | $(0.1-1) \times 10^{-3}$ | $(3-20) \times 10^{-3}$ |
| PDF | $\sim 2 \times 10^{-3}$ | $(1-8) \times 10^{-4}$ | $(0.7-3) \times 10^{-3}$ |
| Other | $\sim 1 \times 10^{-3}$ | $(0.1-2) \times 10^{-3}$ | $(5-9) \times 10^{-3}$ |
| CF electrons | | | |
| Uncertainty | 66–70 GeV | 70–250 GeV | 250–1000 GeV |
| Unfolding | $\sim 2 \times 10^{-2}$ | $(0.5-2) \times 10^{-2}$ | – |
| Energy scale/resolution | $\sim 1 \times 10^{-2}$ | $(0.5-7) \times 10^{-2}$ | – |
| MC statistics | $\sim 1 \times 10^{-2}$ | $(1-7) \times 10^{-3}$ | – |
| Background | $\sim 3 \times 10^{-2}$ | $(0.5-1) \times 10^{-2}$ | – |
| PDF | $\sim 4 \times 10^{-3}$ | $(2-6) \times 10^{-4}$ | – |
| Other | $\sim 1 \times 10^{-3}$ | $(1-5) \times 10^{-4}$ | – |
| Muons | | | |
| Uncertainty | 66–70 GeV | 70–250 GeV | 250–1000 GeV |
| Unfolding | $\sim 1 \times 10^{-2}$ | $(1-4) \times 10^{-3}$ | $\sim 5 \times 10^{-4}$ |
| Energy scale/resolution | $\sim 8 \times 10^{-3}$ | $(3-6) \times 10^{-3}$ | $\sim 5 \times 10^{-3}$ |
| MC statistics | $\sim 5 \times 10^{-3}$ | $(0.1-1) \times 10^{-3}$ | $(2-30) \times 10^{-3}$ |
| PDF | $\sim 2 \times 10^{-3}$ | $(1-8) \times 10^{-4}$ | $(0.3-3) \times 10^{-3}$ |
| Other | $\sim 1 \times 10^{-3}$ | $(0.5-1) \times 10^{-3}$ | $(3-10) \times 10^{-3}$ |

Uncertainties - CMS

Table 2: Summary of experimental systematic uncertainties.

| Source | muons | electrons |
|-----------------------------|---------|-----------|
| MC statistics | 0.00015 | 0.00033 |
| Lepton momentum calibration | 0.00008 | 0.00019 |
| Lepton selection efficiency | 0.00005 | 0.00004 |
| Background subtraction | 0.00003 | 0.00005 |
| Pileup modeling | 0.00003 | 0.00002 |
| Total | 0.00018 | 0.00039 |

| model variation | Muons | Electrons |
|--|---------|-----------|
| Dilepton p_T reweighting | 0.00003 | 0.00003 |
| QCD $\mu_{R/F}$ scale | 0.00011 | 0.00013 |
| POWHEG MiNLO Z+j vs NLO Z model | 0.00009 | 0.00009 |
| FSR model (PHOTOS vs PYTHIA) | 0.00003 | 0.00005 |
| UE tune | 0.00003 | 0.00004 |
| Electroweak ($\sin^2 \theta_{\text{eff}}^{\text{lept}} - \sin^2 \theta_{\text{eff}}^{\text{u,d}}$) | 0.00001 | 0.00001 |
| Total | 0.00015 | 0.00017 |

- PDF uncertainties dominate

Weak mixing angle extraction

- ATLAS:
 - Measure the A_{FB} in bins of M_{ll} with two central electrons (CC), one central and one forward electron (CF) and two muons in the mass range 70-250 GeV.
 - Produce 17 Pythia MC templates for A_{FB} for different values of $\sin^2\theta_{lep}^{eff}$
 - Use a re-weighting technique to obtain fully simulated samples
 - Extract $\sin^2\theta_{lep}^{eff}$ by fitting measured A_{FB} from data to template samples with different $\sin^2\theta_{lep}^{eff}$ values
- CMS :
 - Multivariate likelihood method using variables: decay angle $\cos\theta^*$ invariant mass and rapidity only for the muon events
 - Use analytical prediction for differential cross section, convoluted with analytical models for PDFs, dilution, detector effects
 - Perform unbinned extended maximum likelihood fit to extract the weak mixing angle

AFB and effective weak mixing angle

- The weak mixing angle can be measured from Drell-Yan Z production

$q\bar{q} \rightarrow Z/\gamma^* \rightarrow \ell^+\ell^-$ using the **LO differential cross-section at parton**

level:

$$\frac{d\sigma}{d(\cos\theta)} = \frac{4\pi\alpha^2}{3\hat{s}} \left[\frac{3}{8}A(1 + \cos^2\theta) + B\cos\theta \right]$$

θ is the angle of the neg. lepton relative to the quark momentum in the di-lepton rest frame.

- Linear term** leads to an asymmetry A_{FB} in the polar angle θ distribution of the lepton:

$$A_{FB} = \frac{\sigma_F - \sigma_B}{\sigma_F + \sigma_B} = \frac{\int_0^1 \frac{d\sigma}{d\cos\theta} d\cos\theta - \int_{-1}^0 \frac{d\sigma}{d\cos\theta} d\cos\theta}{\int_0^1 \frac{d\sigma}{d\cos\theta} d\cos\theta + \int_{-1}^0 \frac{d\sigma}{d\cos\theta} d\cos\theta} = \frac{N_F - N_B}{N_F + N_B} = \frac{3B}{8A}$$

$\cos\theta > 0$: Forward event
 $\cos\theta < 0$: Backward event

$$A = Q_l^2 Q_q^2 + 2Q_l Q_q g_V^q g_V^l \text{Re}(\chi(s)) + (g_V^{l^2} + g_A^{l^2})(g_V^{q^2} + g_A^{q^2})|\chi(s)|^2$$

$$B = \frac{3}{2}g_A^q g_A^l (Q_l Q_q \text{Re}(\chi(s)) + 2g_V^q g_V^l |\chi(s)|^2)$$

the weak mixing angle can be extracted by A_{FB} at the M_Z scale

- $\sin^2\theta_w$ at tree level is defined as: $1 - m_w^2/m_Z^2$. Including higher order EW corrections the tree level expression of the couplings g_V and g_A are modified. The $\sin^2\theta_{\text{eff}}$ is related to the EW coupling g_V

$$\bar{g}_V^f = \sqrt{\rho_f} (T_f^3 - 2Q_f \sin^2\theta_{\text{eff}}), \quad \text{with } \sin^2\theta_{\text{eff}} = \kappa_f \sin^2\theta_W$$

- The EW corrections are absorbed into ρ_f and κ_f